Unprecedented collateral sensitivity for cisplatin-resistant lung cancer cells presented by new ruthenium organometallic compounds

Ricardo G. Teixeira[a], Dimas C. Belisario[b], Xavier Fontrodona[c], Isabel Romero[c], Ana Isabel Tomaz[a] , M. Helena Garcia[a], Chiara Riganti[b], Andreia Valente[a,*]

[a] Centro de Química Estrutural and Departamento de Química e Bioquímica, Faculdade de Ciências, Universidade de Lisboa, Campo Grande, 1749-016 Lisboa, Portugal.

[b] Department of Oncology, University of Torino, Torino, Italy.

[c] Departament de Química and Serveis Tècnics de Recerca, Universitat de Girona, C/ M. Aurèlia Campmany, 69, E-17003 Girona, Spain.

Corresponding Authors

*E-mail: amvalente@ fc.ul.pt

Table of Contents

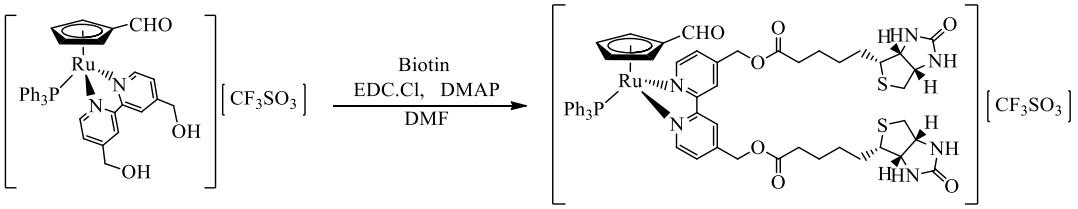

Scheme S1. Synthesis of compound **4**.

[redacted]

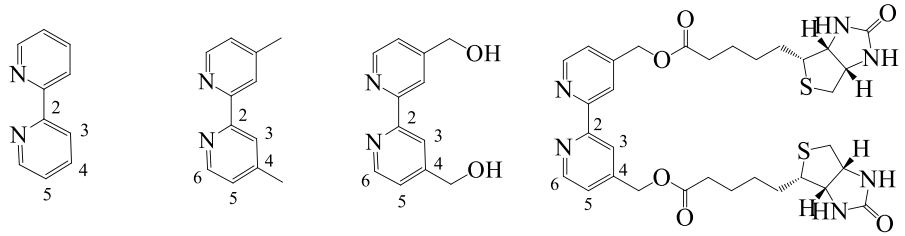

Scheme S2. Synthesis route of compounds **1–3** and **5-8**; all compounds are numbered for NMR assignments. ** Compound 8 was not studied in this work.

S1. ESI mass spectra

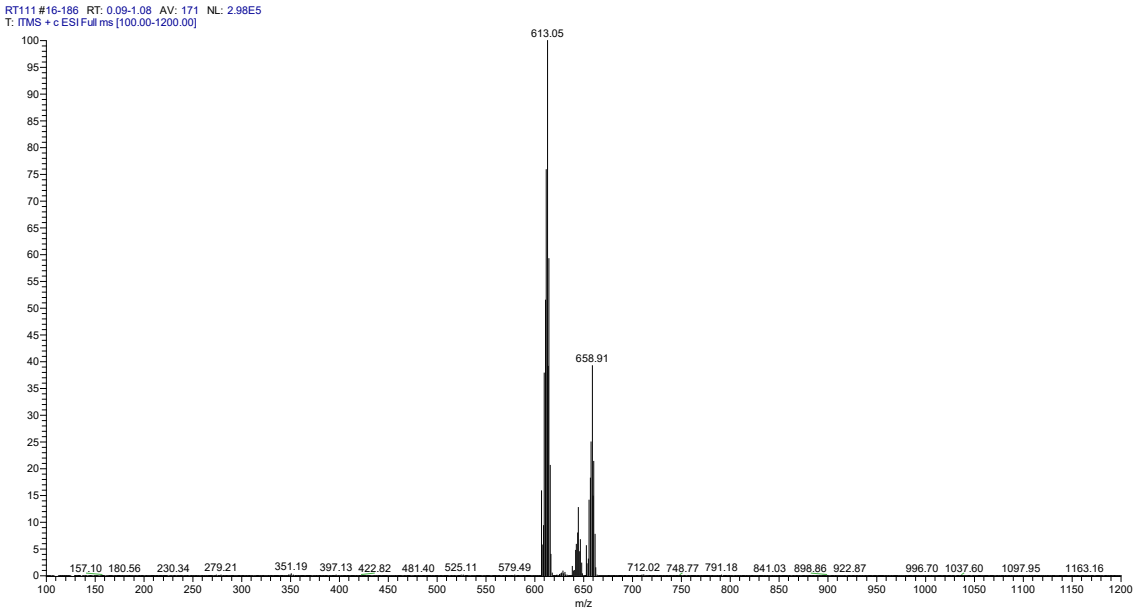

Figure S1. ESI-MS spectrum of complex **1** (positive detection mode).

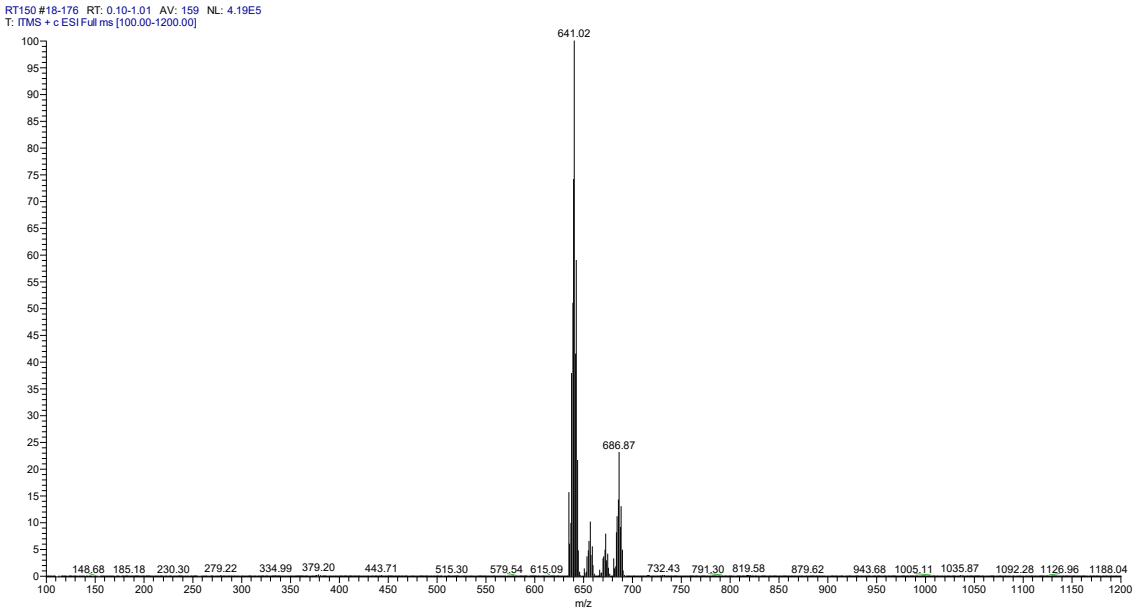

Figure S2. ESI-MS spectrum of complex **2** (positive detection mode).

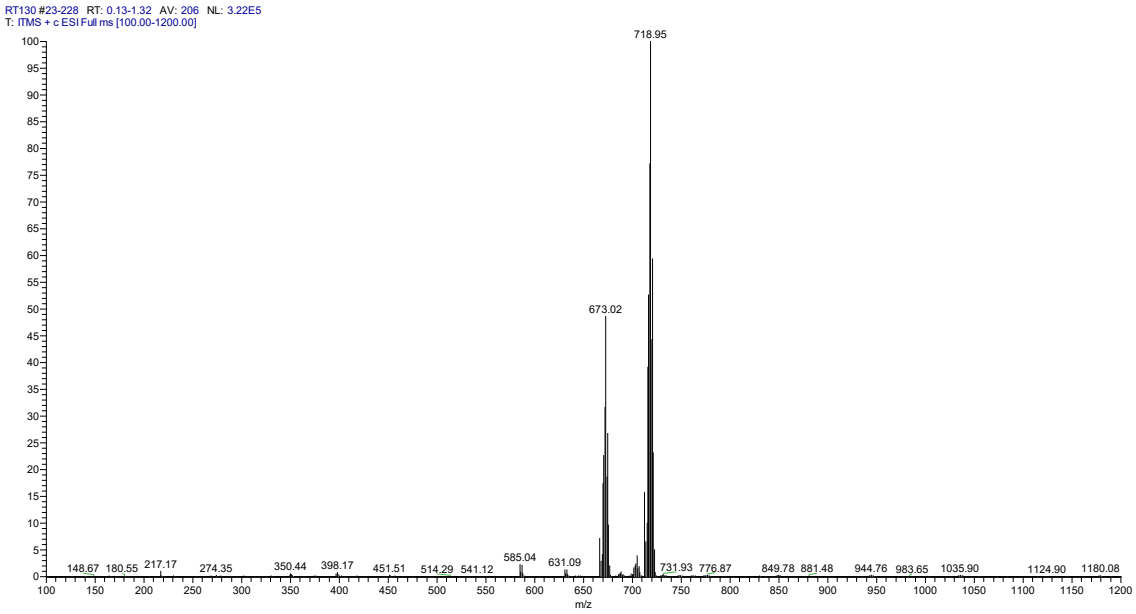

Figure S3. ESI-MS spectrum of complex **3** (positive detection mode).

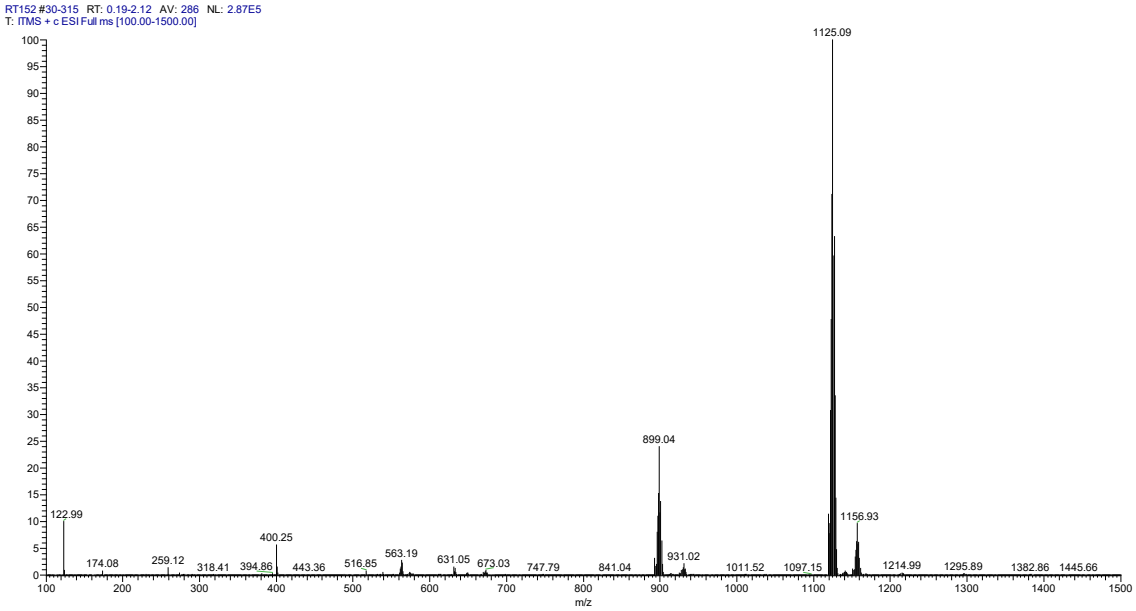

Figure S4. ESI-MS spectrum of complex **4** (positive detection mode).

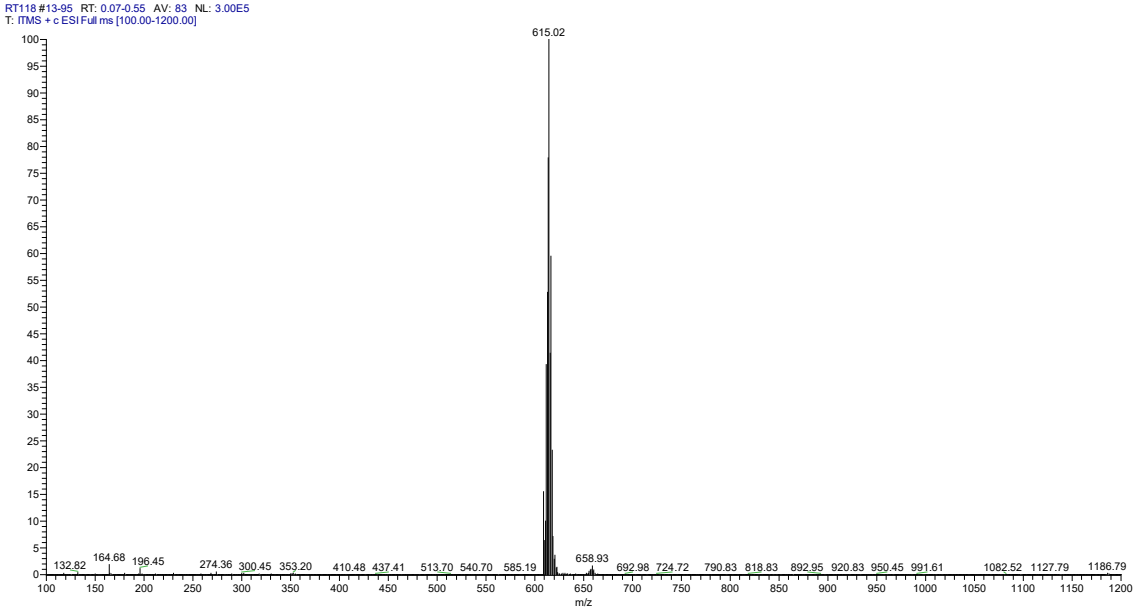

Figure S5. ESI-MS spectrum of complex **5** (positive detection mode).

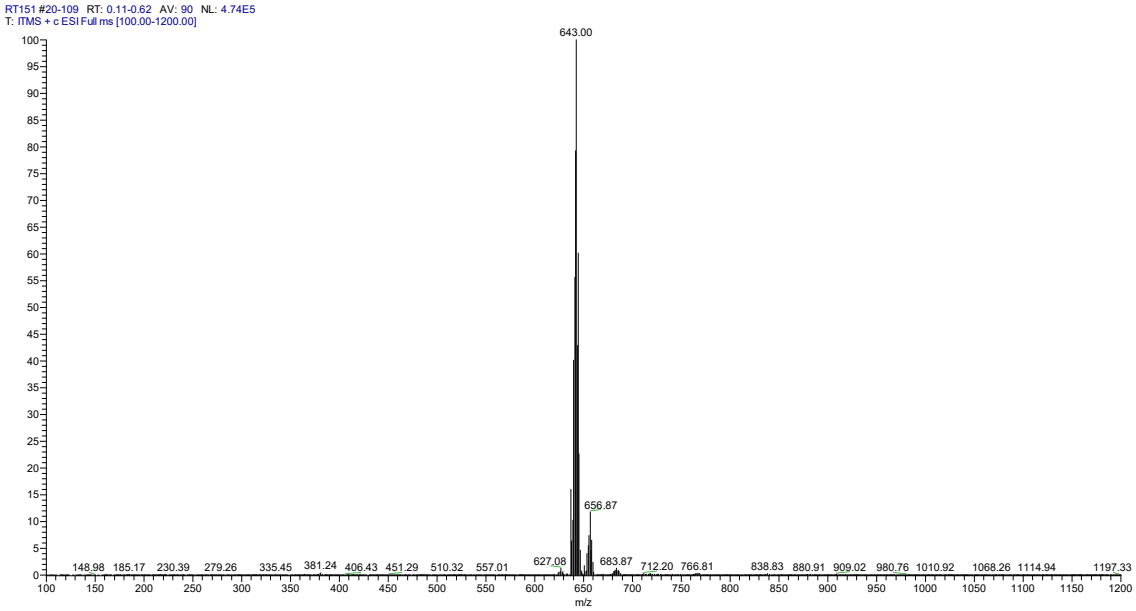

Figure S6. ESI-MS spectrum of complex **6** (positive detection mode).

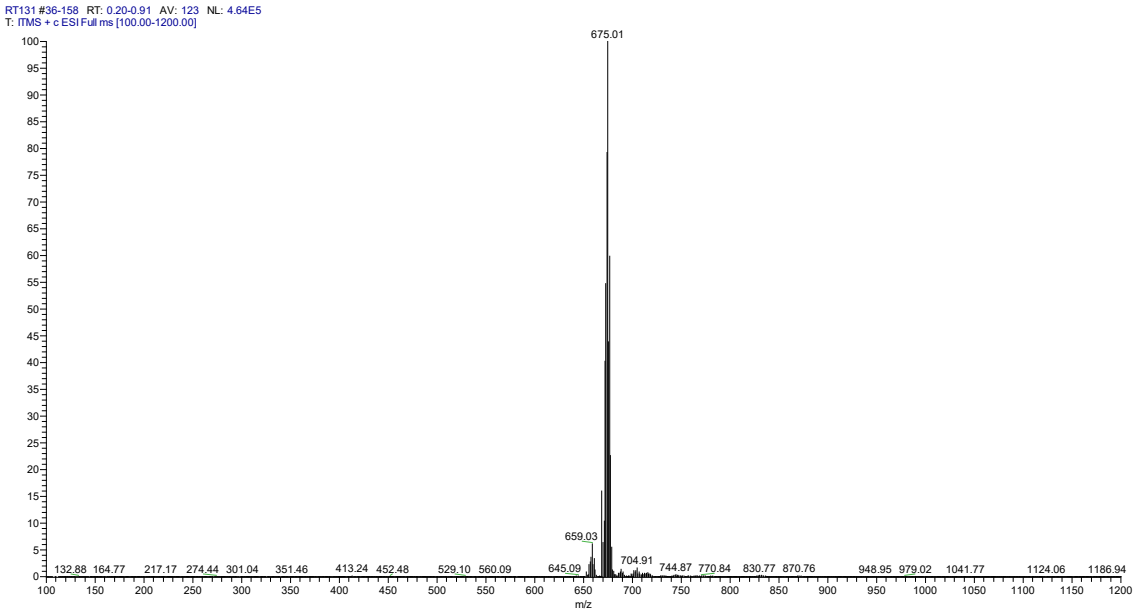

Figure S7. ESI-MS spectrum of complex **7** (positive detection mode).

S2. NMR spectra

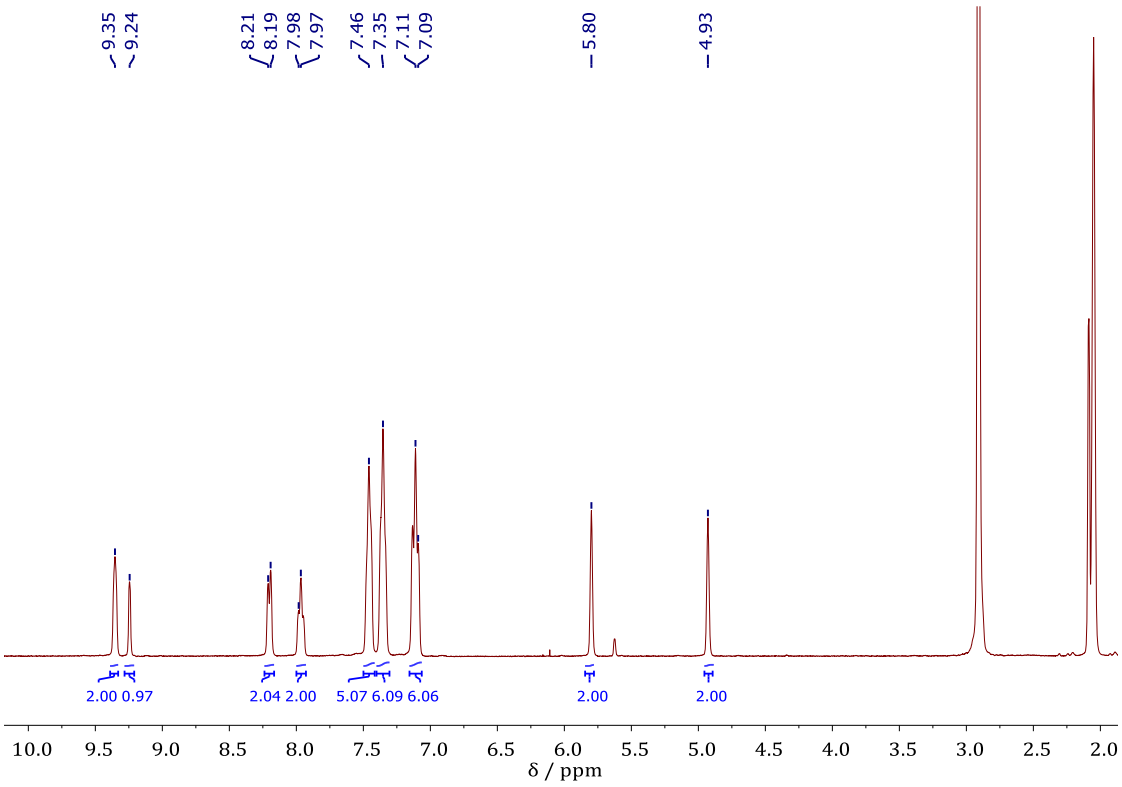

Figure S8. ^{1}H-NMR spectrum of complex **1** in acetone-d_6 at 298 K.

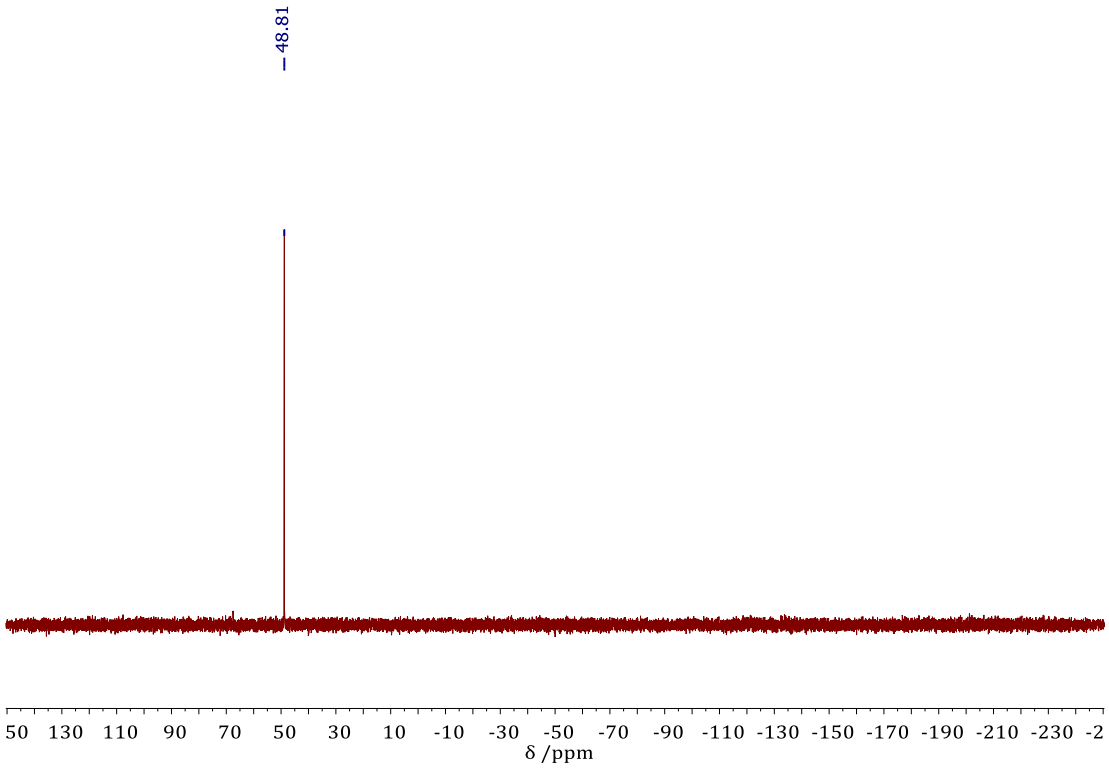

Figure S9. ^{31}P{^{1}H}-NMR spectrum of complex **1** in acetone-d_6 at 298 K.

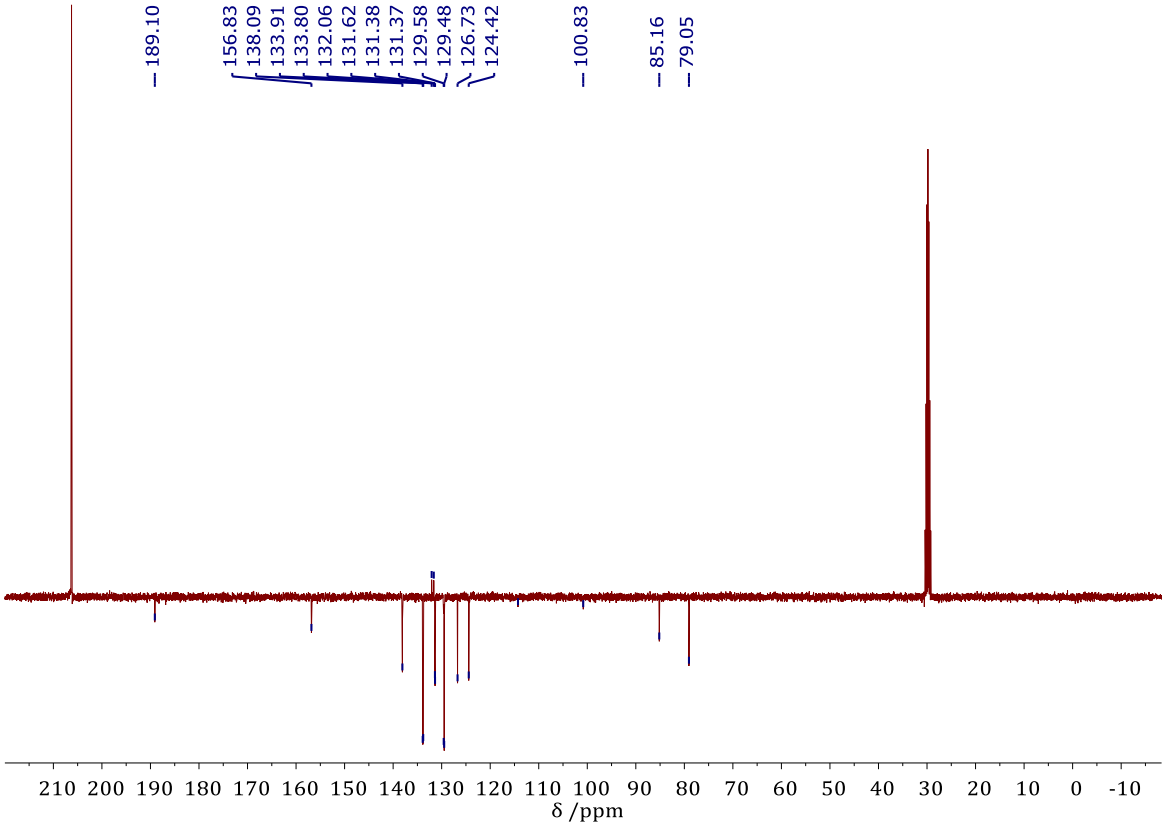

Figure S10. APT $^{13}C\{^{1}H\}$-NMR spectrum of complex **1** in acetone-d_6 at 298 K.

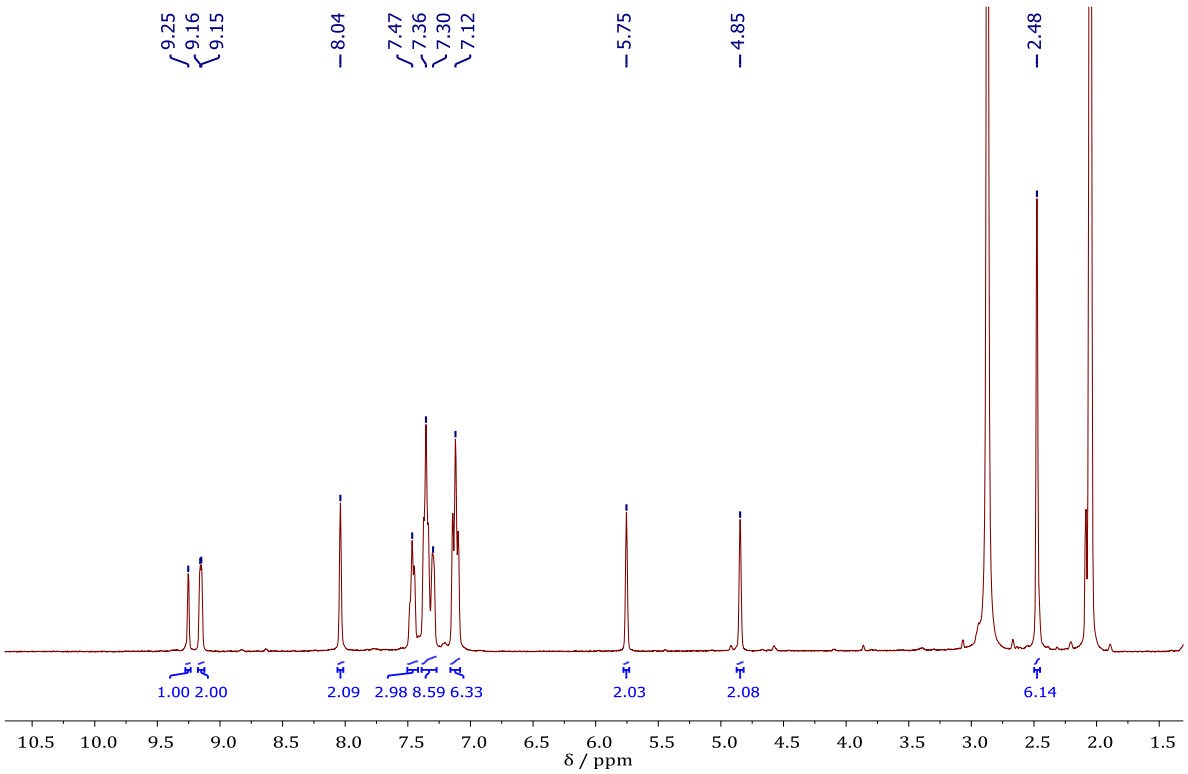

Figure S11. ^{1}H-NMR spectrum of complex **2** in acetone-d_6 at 298 K.

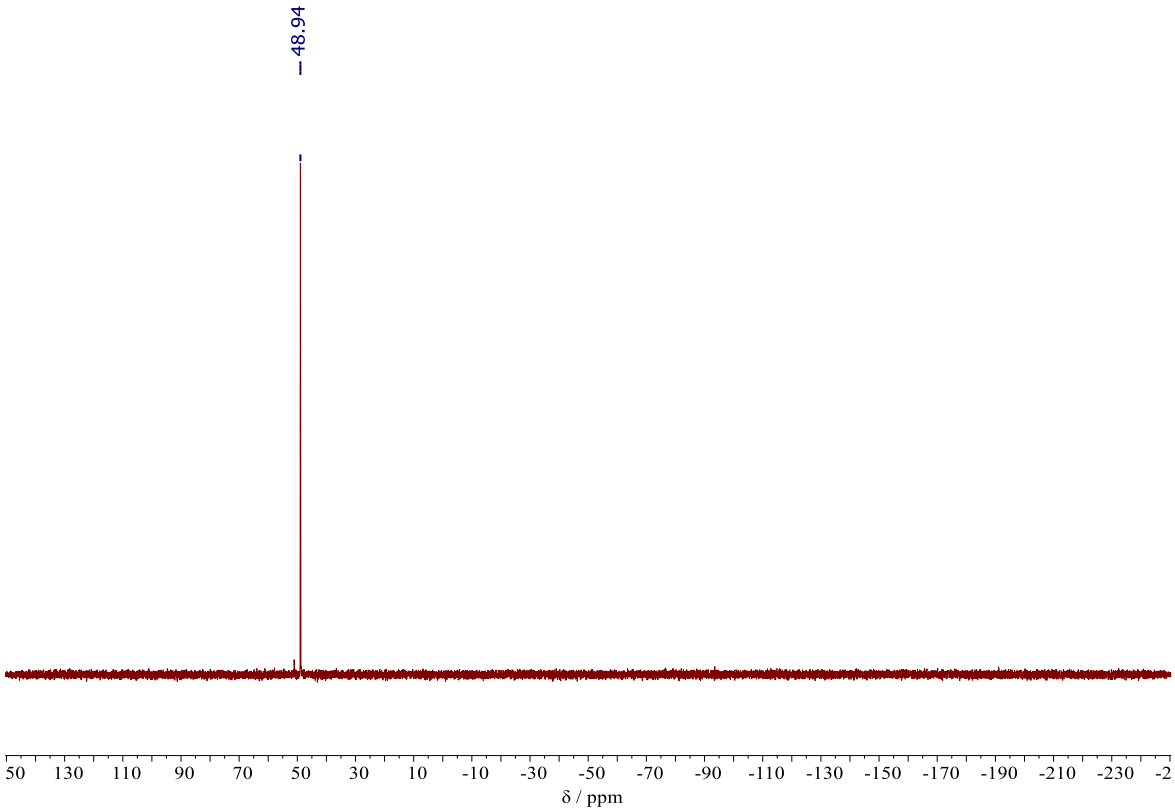

Figure S12. $^{31}P\{^{1}H\}$-NMR spectrum of complex **2** in acetone-d_6 at 298 K.

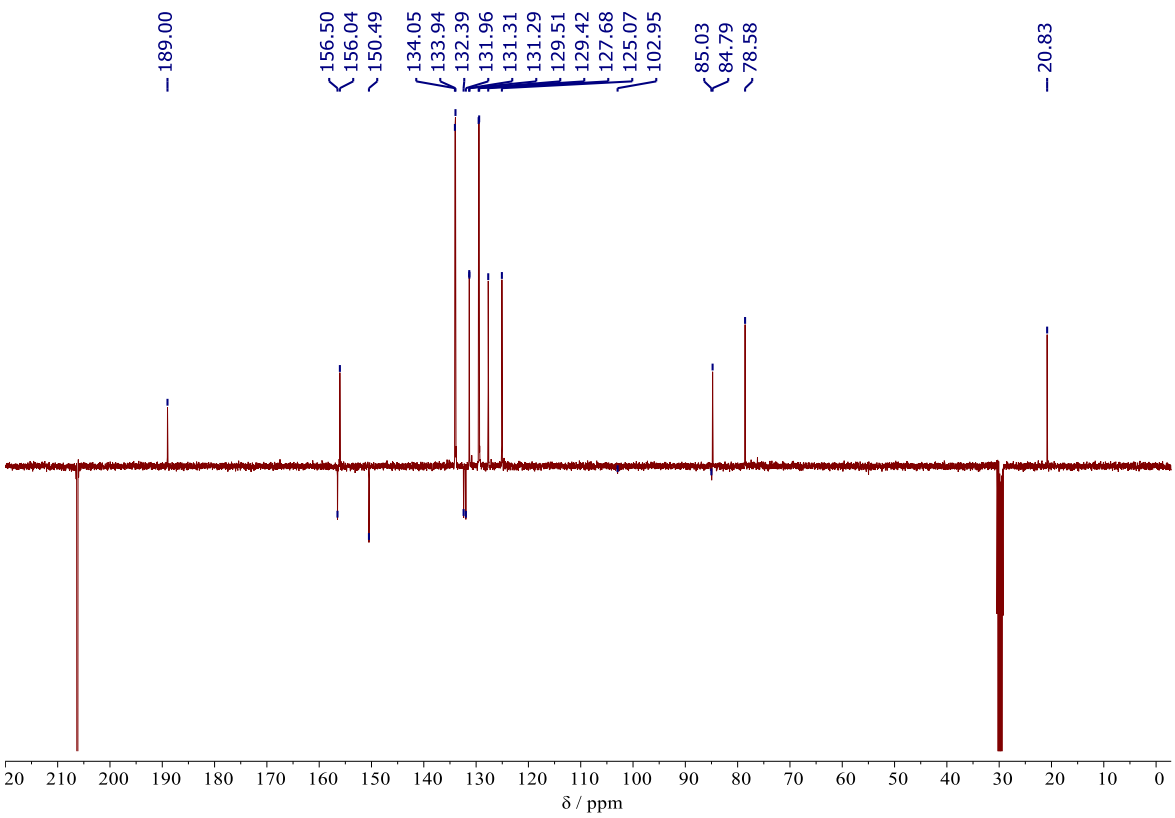

Figure S13. APT $^{13}C\{^{1}H\}$-NMR spectrum of complex **2** in acetone-d_6 at 298 K.

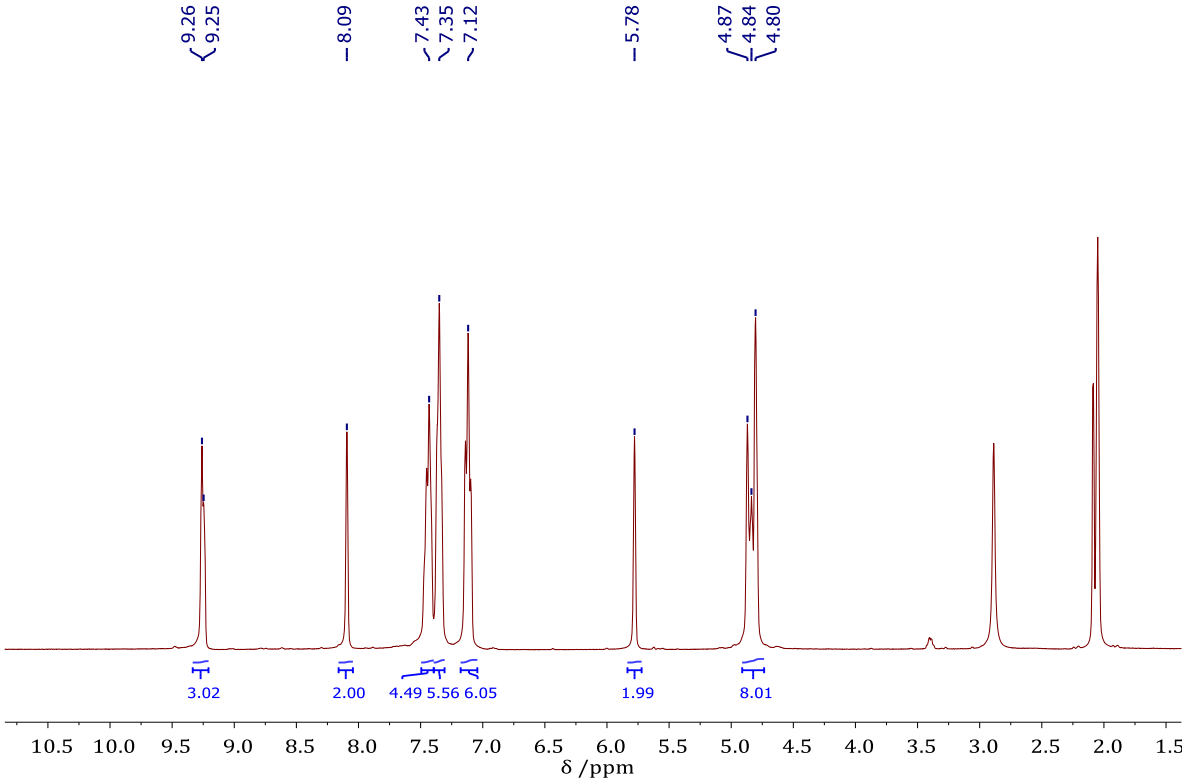

Figure S14. ^{1}H-NMR spectrum of complex **3** in acetone-d_6 at 298 K.

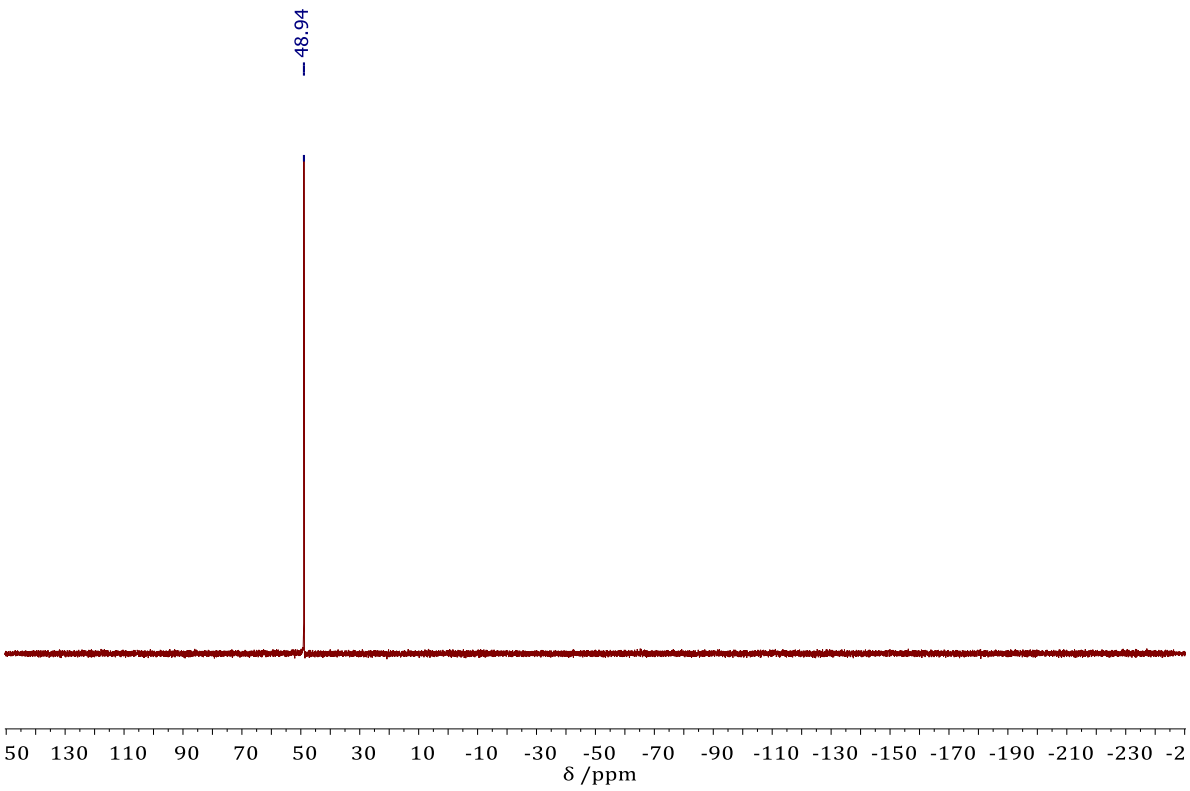

Figure S15. ^{31}P{^{1}H}-NMR spectrum of complex **3** in acetone-d_6 at 298 K.

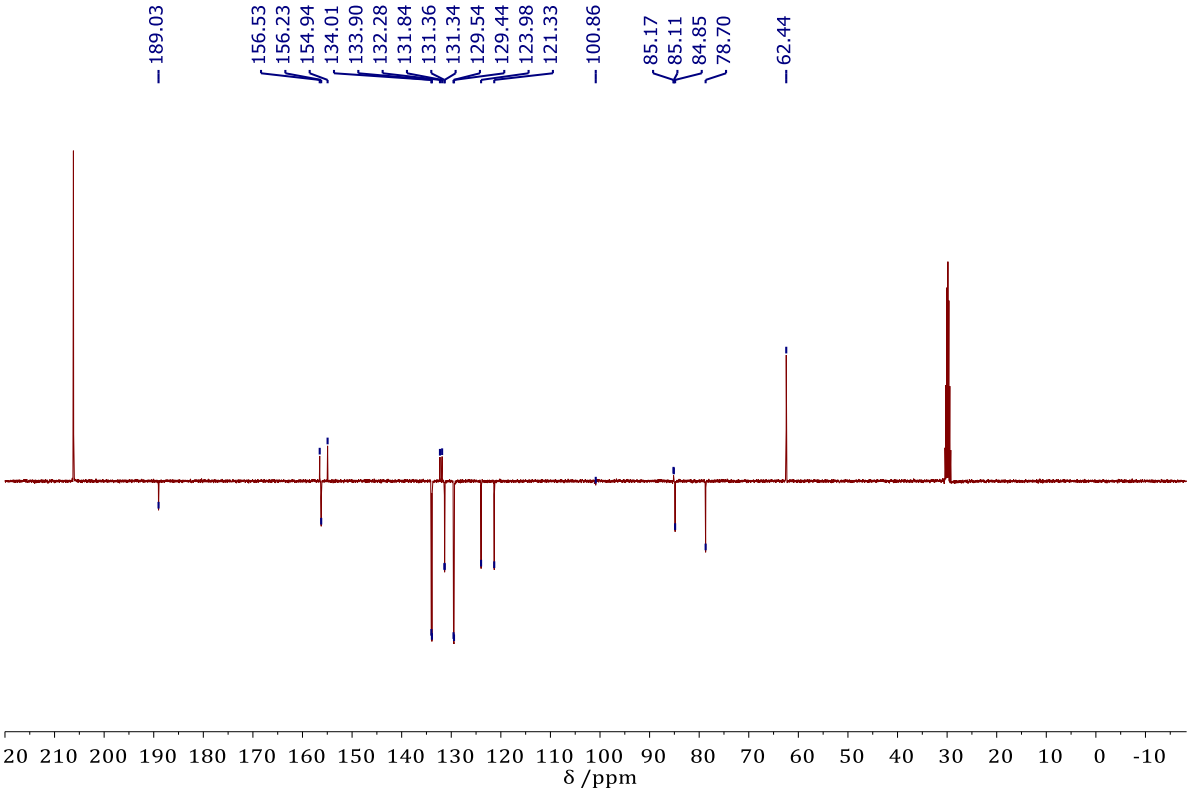

Figure S16. APT $^{13}C\{^{1}H\}$-NMR spectrum of complex **3** in acetone-d_6 at 298 K.

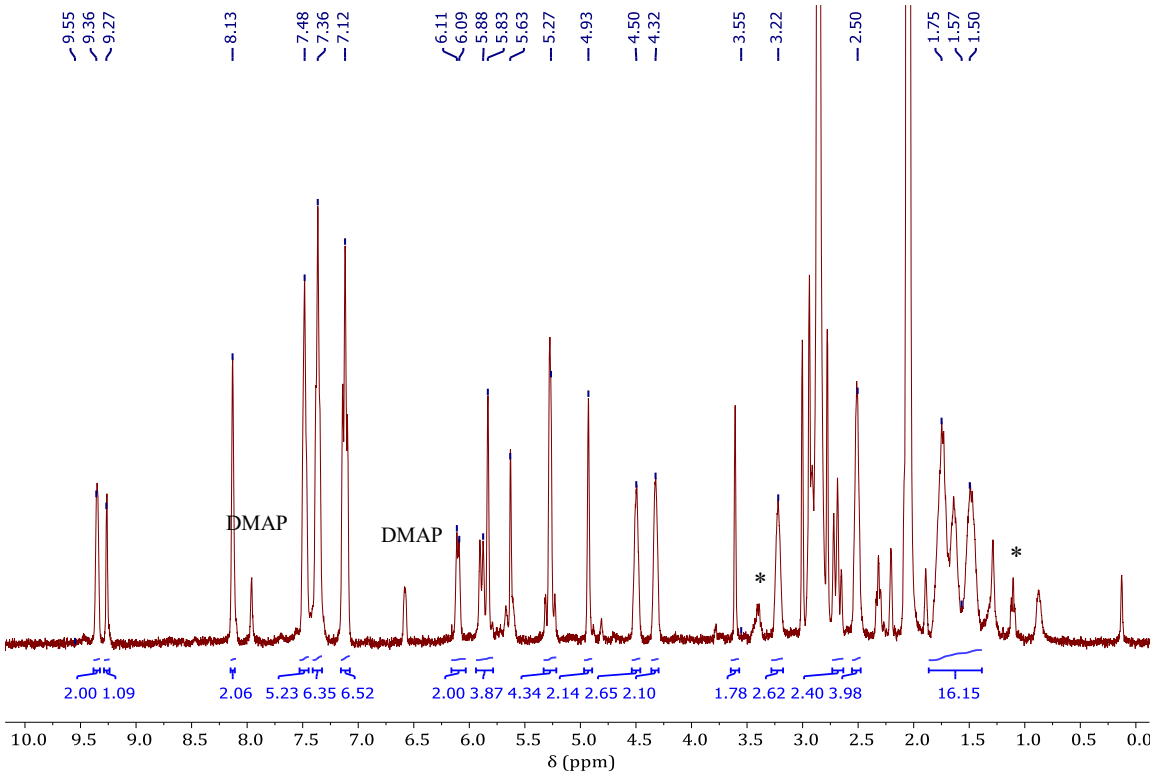

Figure S17. ^{1}H-NMR spectrum of complex **4** in acetone-d_6 at 298 K.

* residual diethyl ether

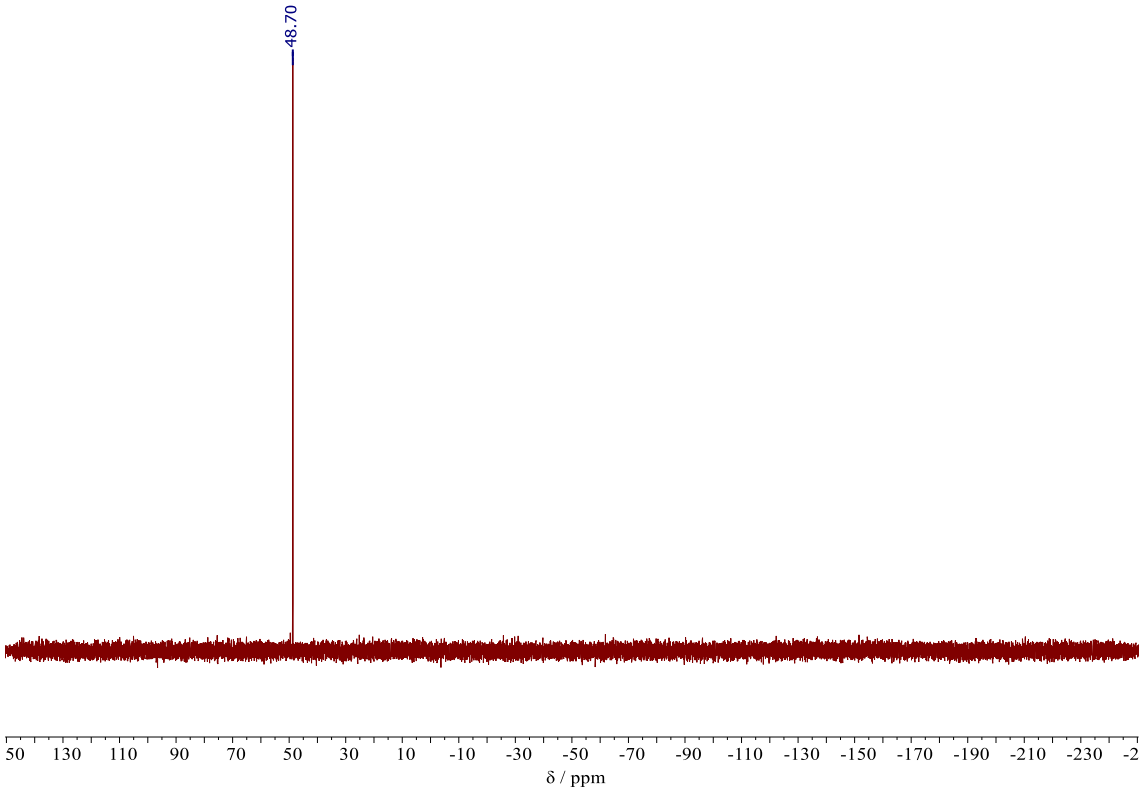

Figure S18. $^{31}P\{^{1}H\}$-NMR spectrum of complex **4** in acetone-d_6 at 298 K.

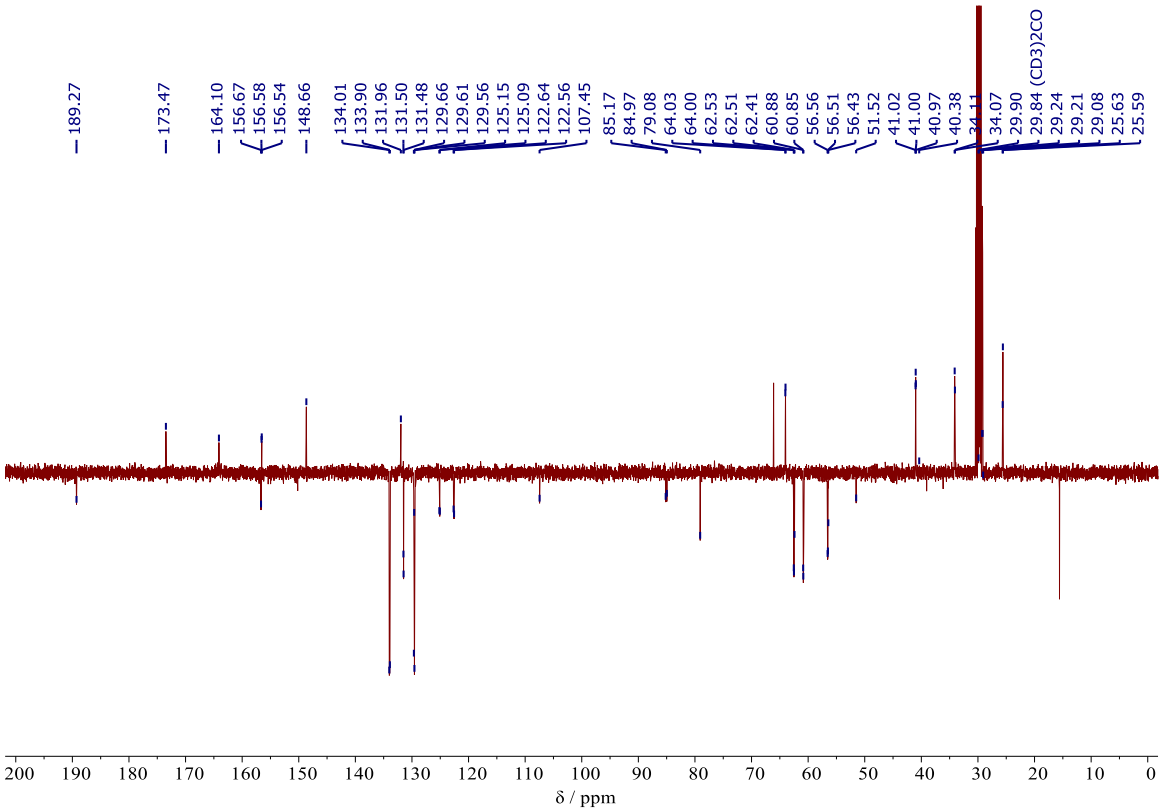

Figure S19. APT $^{13}C\{^{1}H\}$-NMR spectrum of complex **4** in acetone-d_6 at 298 K.

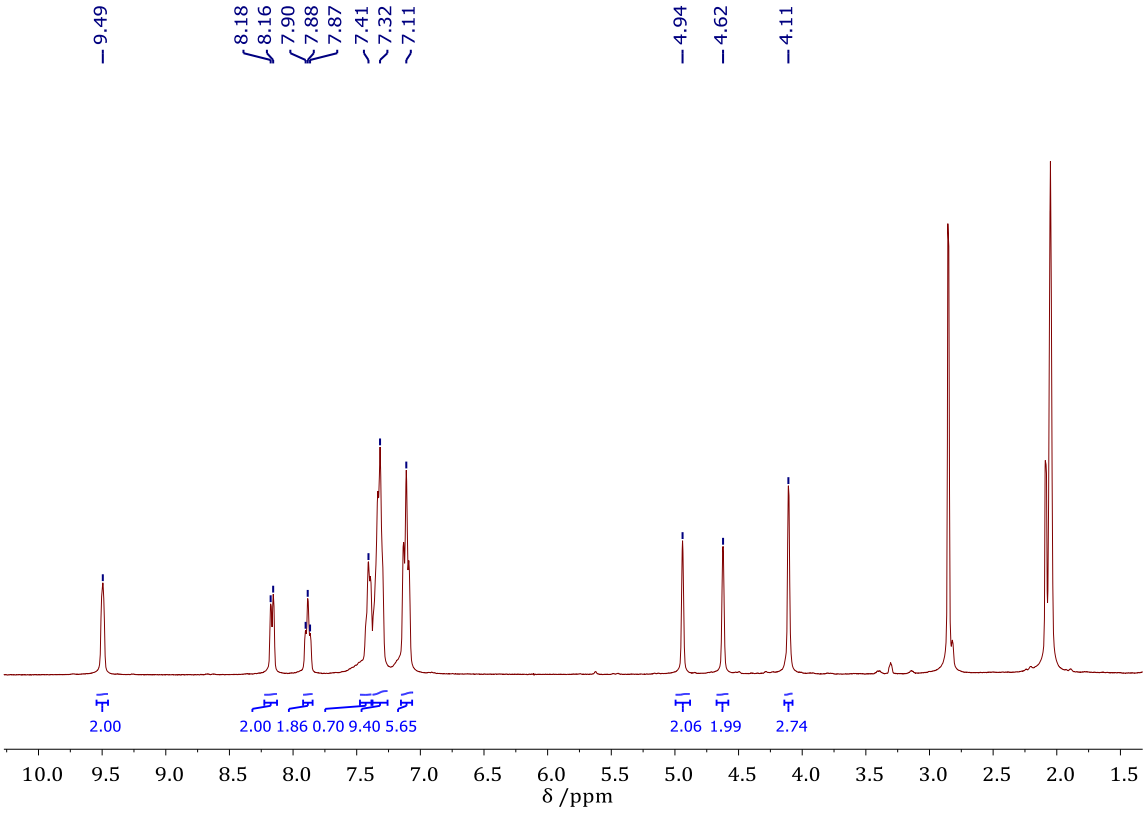

Figure S20. ^{1}H-NMR spectrum of complex **5** in acetone-d$_6$ at 298 K.

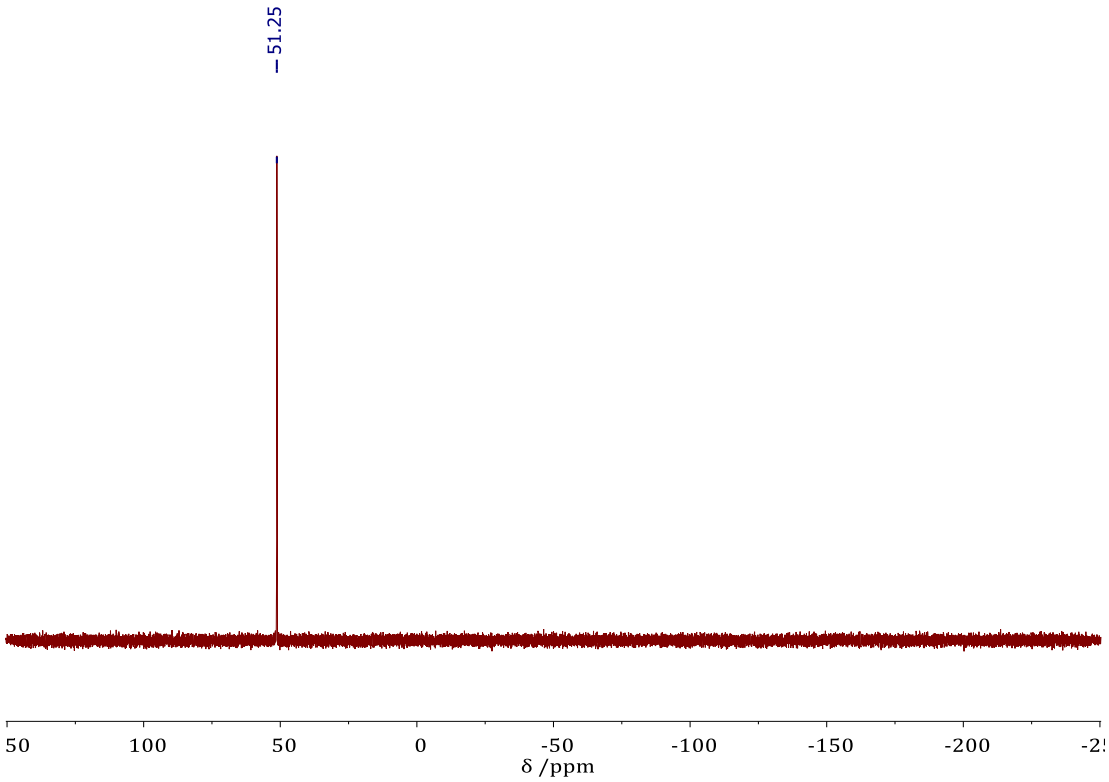

Figure S21. ^{31}P{^{1}H}-NMR spectrum of complex **5** in acetone-*d*$_6$ at 298 K.

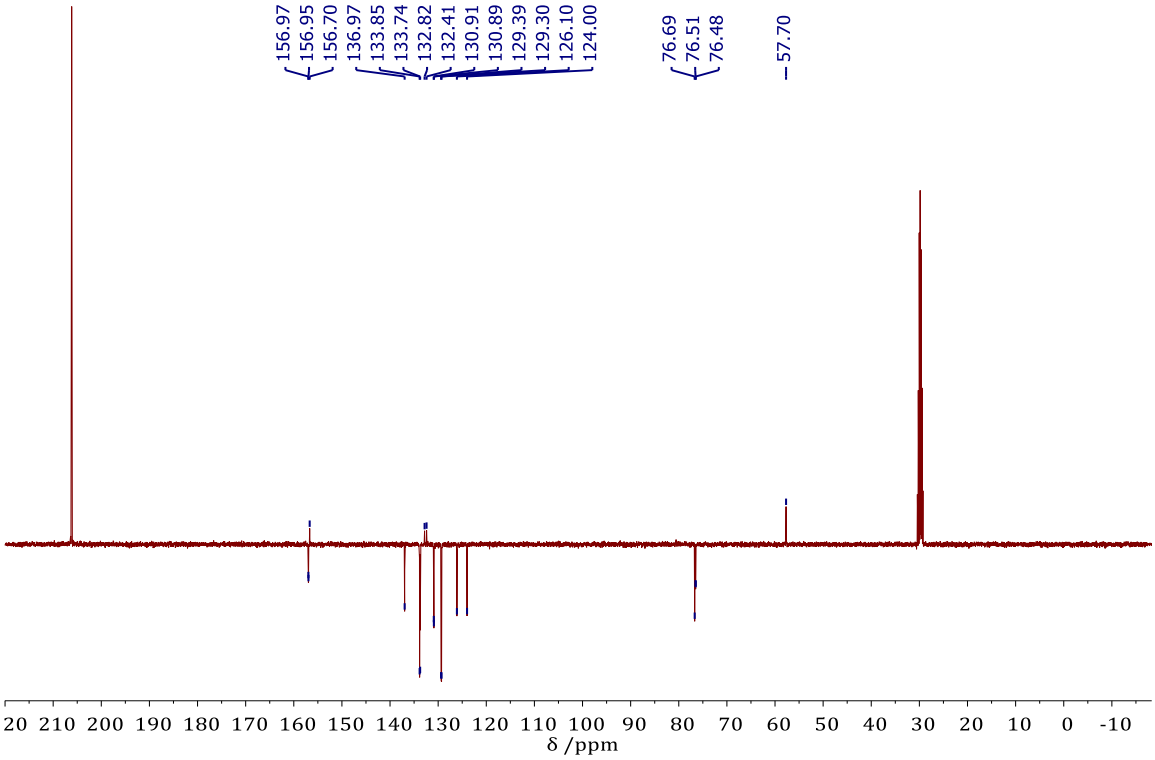

Figure S22. APT $^{13}C\{^{1}H\}$-NMR spectrum of complex **5** in acetone-d_6 at 298 K.

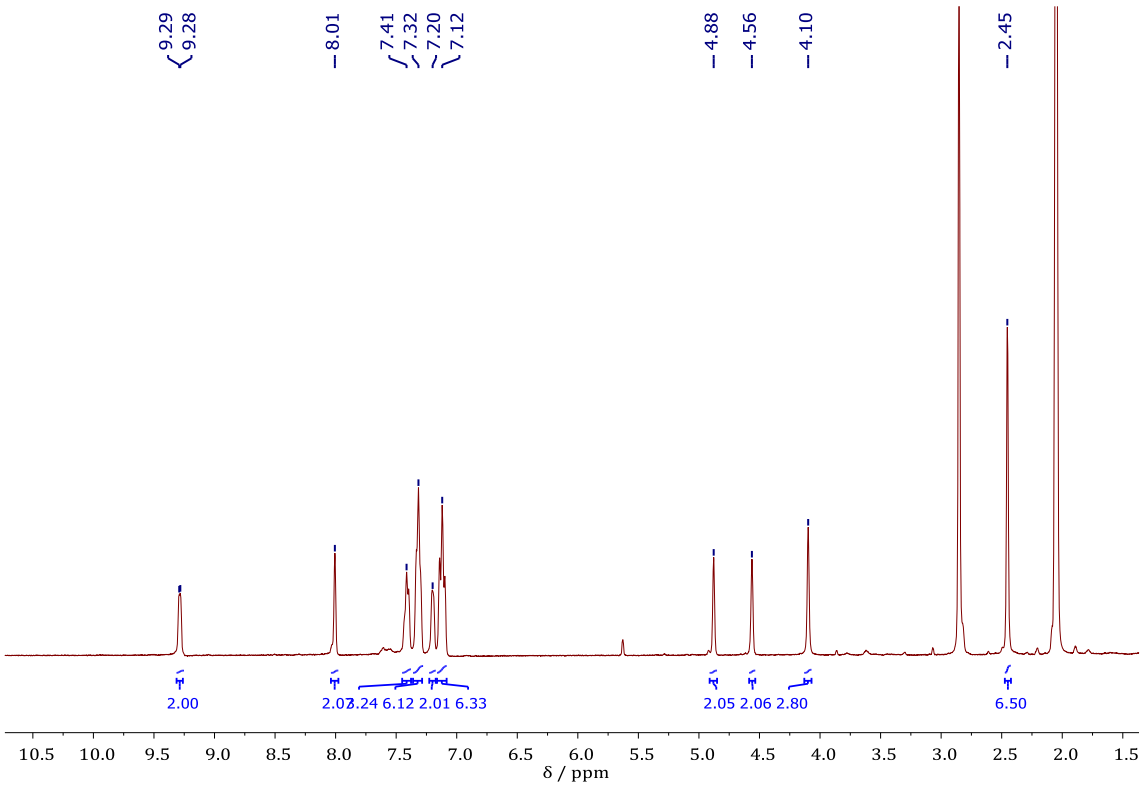

Figure S23. ^{1}H-NMR spectrum of complex **6** in acetone-d_6 at 298 K.

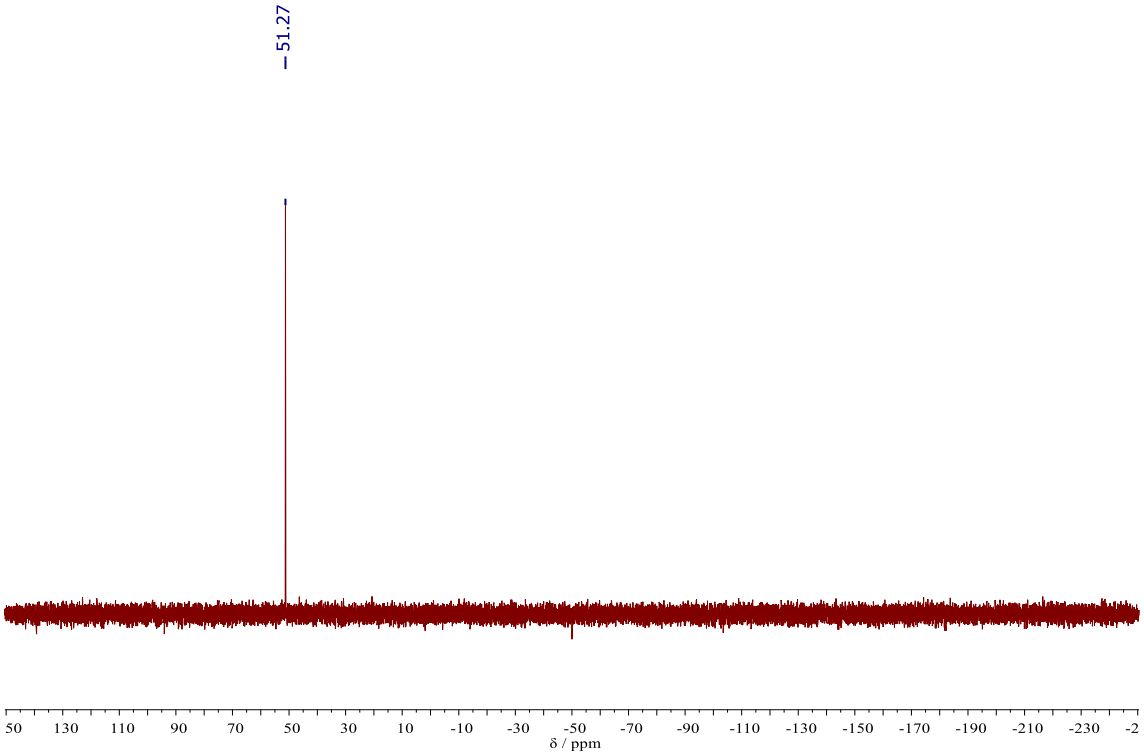

Figure S24. $^{31}P\{^{1}H\}$-NMR spectrum of complex **6** in acetone-d_6 at 298 K.

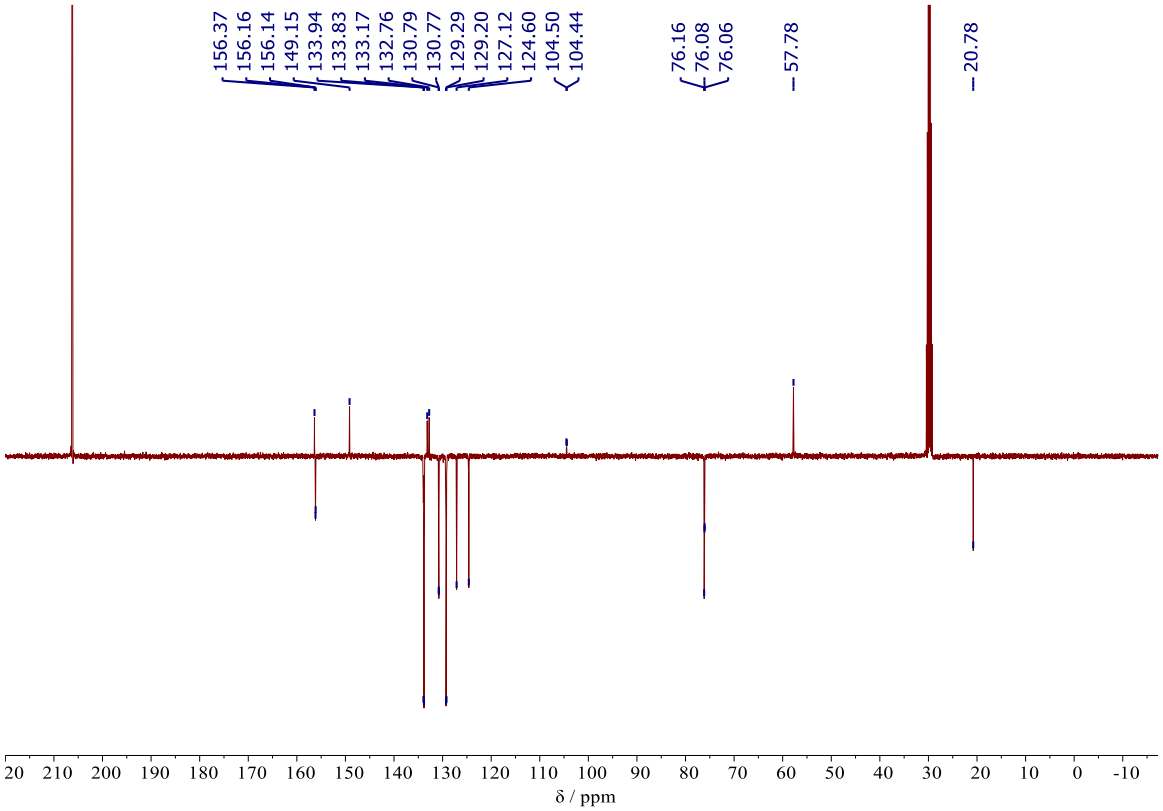

Figure S25. APT $^{13}C\{^{1}H\}$-NMR spectrum of complex **6** in acetone-d_6 at 298 K.

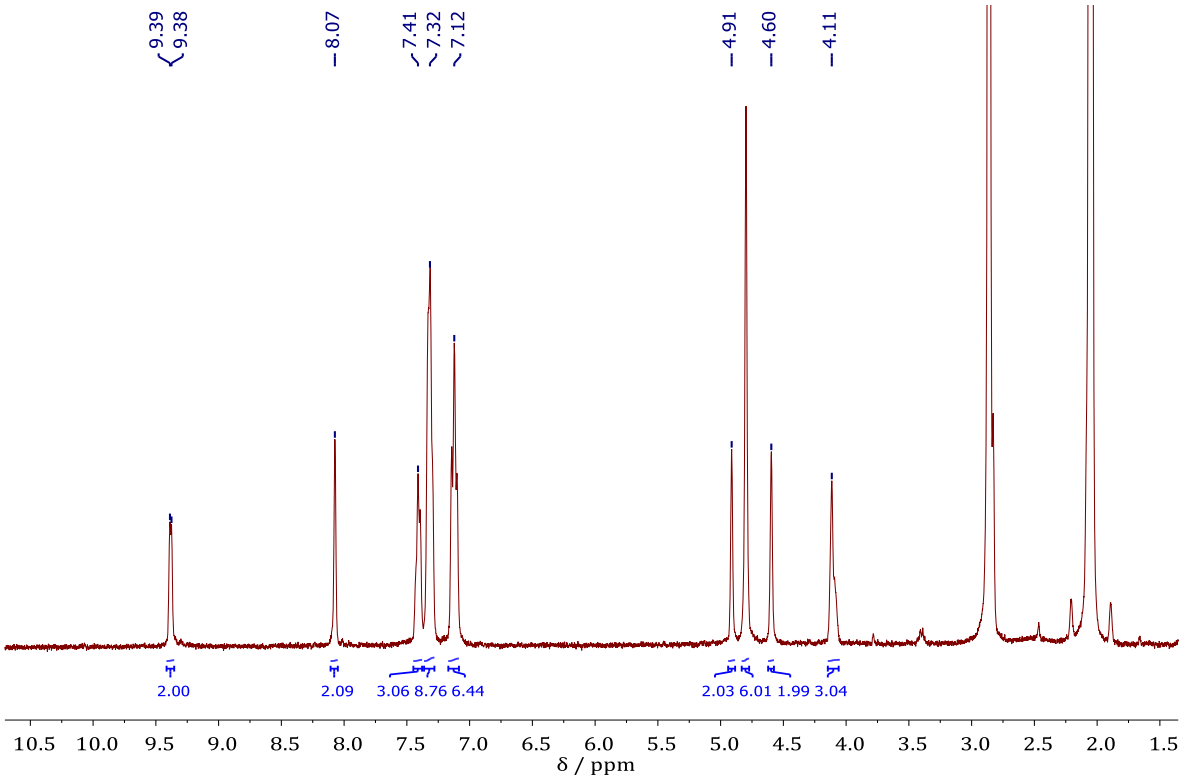

Figure S26. ^{1}H-NMR spectrum of complex **7** in acetone-d_6 at 298 K.

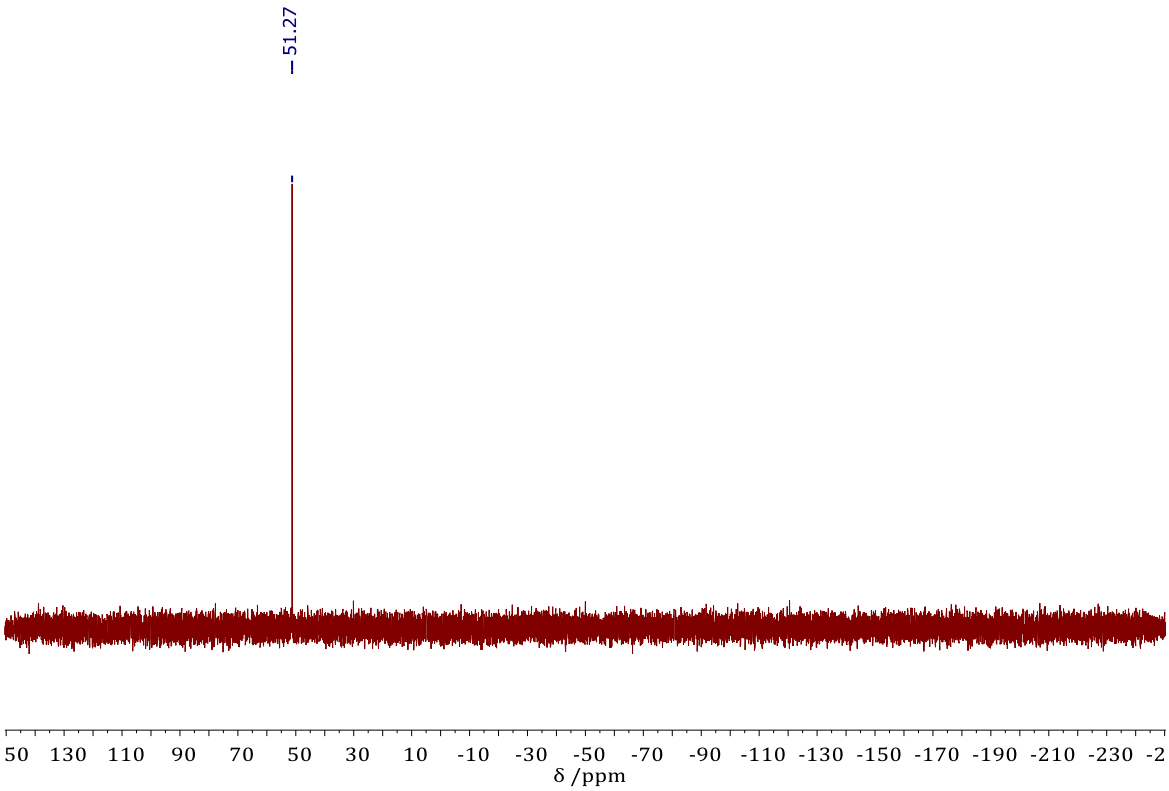

Figure S27. ^{31}P{^{1}H}-NMR spectrum of complex **7** in acetone-d_6 at 298 K.

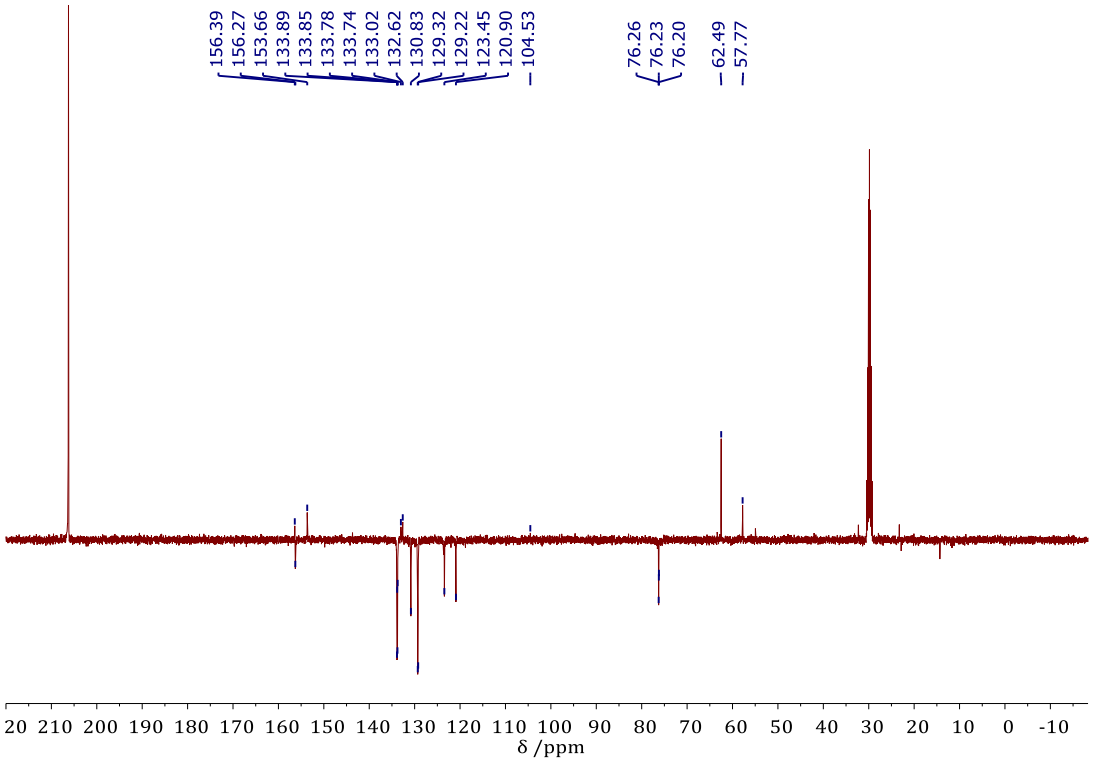

Figure S28. APT $^{13}C\{^{1}H\}$-NMR spectrum of complex **7** in acetone-d_6 at 298 K.

S3. Electronic data

Table S1. Optical spectral data for compounds **1**–**7** in dichloromethane and dimethylsufoxide. Measurements were performed at room temperature using 10^{-4}–10^{-6} M solutions. (Sh = Shoulder).

Compound	**λ_{max} /nm (ε x 10^3 / $M^{-1}cm^{-1}$)**	
	Dichloromethane	**Dimethylsulfoxide**
1	289 (21.71), 357 (Sh), 409 (Sh), 457 (Sh)	289 (24.49), 362 (6.46), 415 (Sh)
2	290 (26.10), 366 (6.91), 412 (Sh)	289 (26.27), 371 (7.21), 412 (Sh)
3	277 (Sh), 289 (28.43), 379 (7.43), 451 (Sh)	290 (27.15), 366 (7.27), 416 (Sh)
4	291 (12.59), 345 (Sh), 416 (2.39), 479 (Sh)	293 (47.69), 358 (11.94), 414(Sh) 468 (Sh)
5	291 (24.89), 348 (Sh), 423 (4.38), 486 (Sh)	292 (16.59), 344 (Sh), 411 (2.93), 483 (Sh)
6	287 (29.20), 345 (Sh), 417 (5.28), 470 (Sh)	291 (4.11), 351 (Sh), 418 (6.86), 472 (Sh).
7	292 (8.16), 367 (Sh), 416 (1.75), 467 (Sh)	255 (Sh), 292 (5.67), 348 (Sh), 416 (1.02), 478 (Sh)

S4. X-ray crystallographic structure determination

Table S2. Crystallographic data and structural refinement details for compounds **1**, **2** and **3**.

	Compound 1	**Compound 2**	**Compound 3**
Empirical formula	$C_{35}H_{28}F_3N_2O_4PRuS$	$C_{38}H_{34}Cl_2F_3N_2O_4PRuS$	$C_{37}H_{32}F_3N_2O_6PRuS$
Formula weight	761.69	874.67	821.74
Temperature (K)	100(2)	100(2)	100(2)
Crystal system	Monoclinic	Triclinic	Monoclinic
space group	C 2/c	P-1	P 2_1/c
a (Å)	31.2279(13)	10.807(8)	12.6767(4)
b (Å)	9.3748(4)	11.451(8)	14.7750(5)
c (Å)	21.6058(8)	16.422(12)	19.1689(6)
β (deg)	92.8700	α = 74.05(2); β = 72.092(18); γ = 77.223(17)	108.3440(10)
Volume ($Å^3$)	6317.3(4)	1838.(2)	3407.86(19)
Z	8	2	4
Calculated density (g cm^{-3})	1.602	1.580	1.602
Absorption coeficient (mm^{-1})	0.674	0.731	0.636
Goodness-of-fit	1.060	1.109	1.093
R_1 [I>2σ(I)]	0.0236	0.0321	0.0248
wR_2 [I>2σ(I)]	0.0588	0.0637	0.0555

Table S3. Crystallographic data and structural refinement details for compounds **5**, **6** and **7**.

	Compound 5	**Compound 6**	**Compound 7**
Empirical formula	$C_{35}H_{30}F_3N_2O_4PRuS$	$C_{37}H_{34}F_3N_2O_4PRuS$	$C_{37}H_{34}F_3N_2O_6PRuS$
Formula weight (g mol^{-1})	763.71	791.76	823.76
Temperature (K)	100(2)	100(2)	100(2)
Crystal system	Monoclinic	Monoclinic	Monoclinic
space group	P 2_1/n	P 2_1/n	P 2_1/c
a (Å)	12.995(8)	12.8677(4)	16.356(15)
b (Å)	13.774(9)	14.2849(5)	10.914(10)
c (Å)	18.311(12)	19.4057(6)	20.074(18)
β (deg)	105.75(2)	105.8660(10)	108.95(3)
Volume ($Å^3$)	3154.(4)	3431.14(19)	3389.(5)
Z	4	4	4
Calculated density (g cm^{-3})	1.608	1.533	1.614
Absorption coeficient (mm^{-1})	0.676	0.624	0.639
Goodness-of-fit	1.051	1.115	1.156
R_1 [I>2σ(I)]	0.0265	0.0390	0.0491
wR_2 [I>2σ(I)]	0.0554	0.0915	0.1153

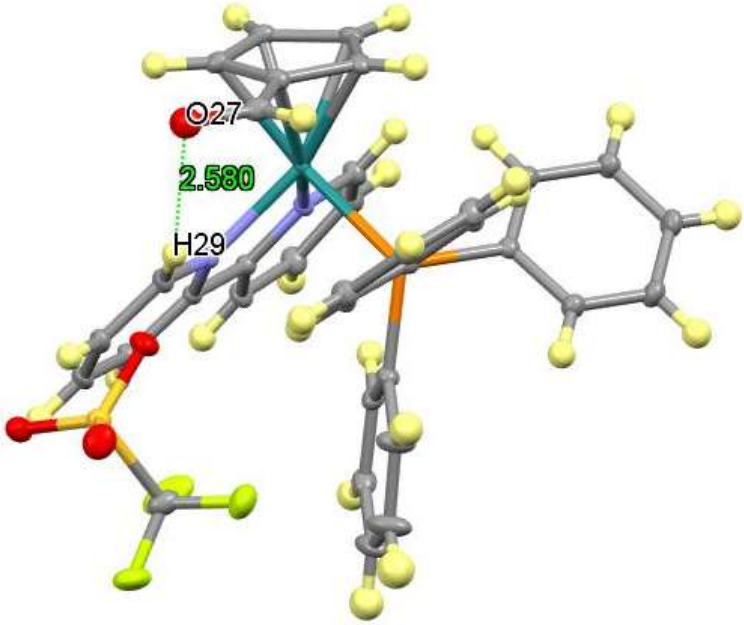

Figure S29. X-ray structure of **1** showing the intramolecular hydrogen bond.

A)

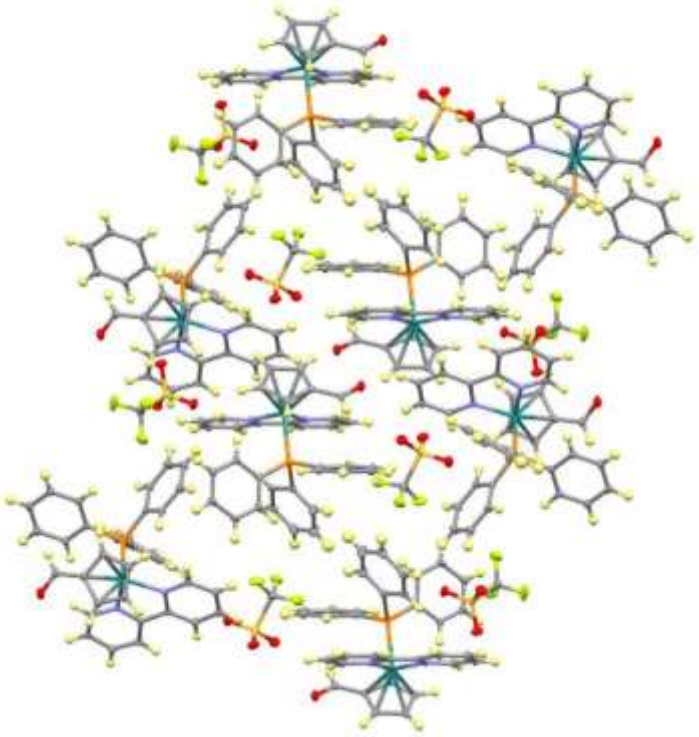

B)

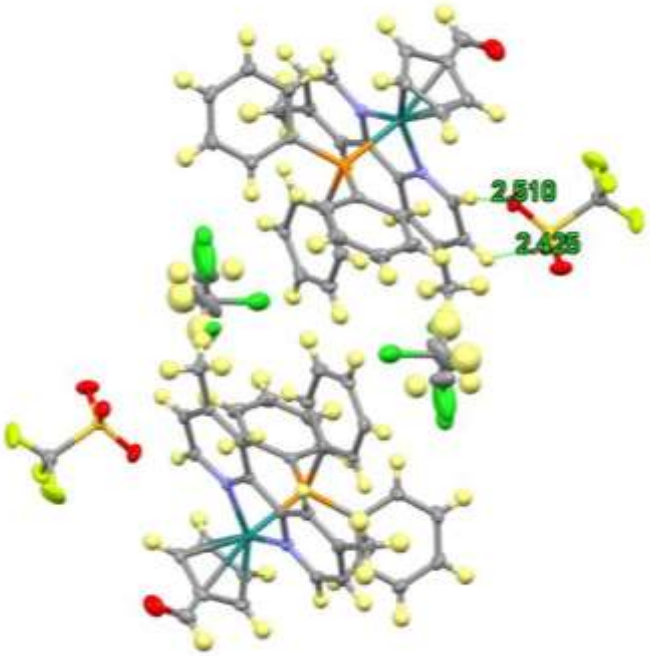

C)

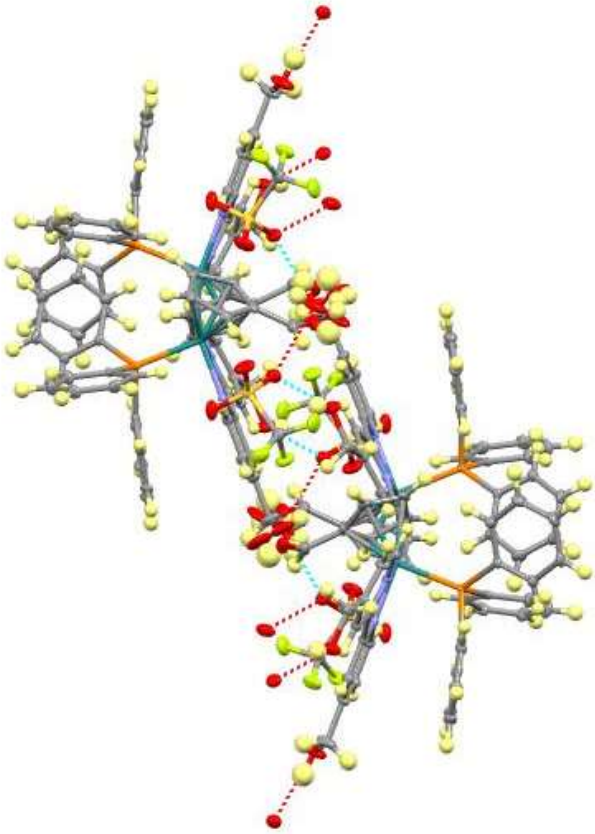

D)

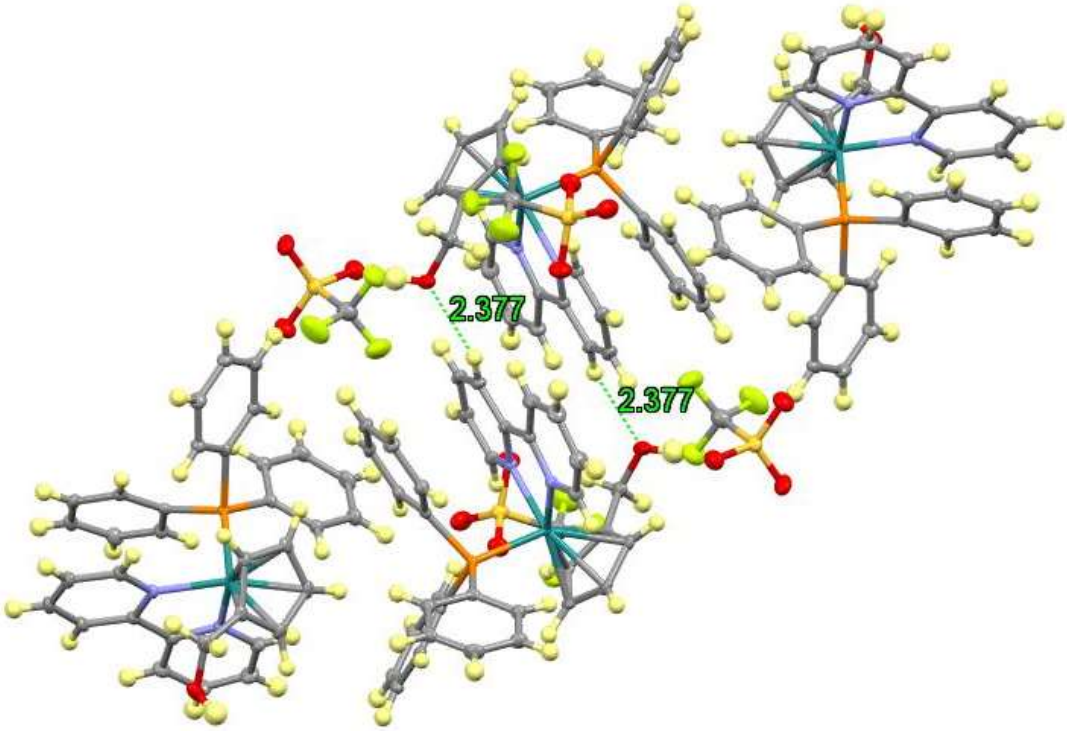

E)

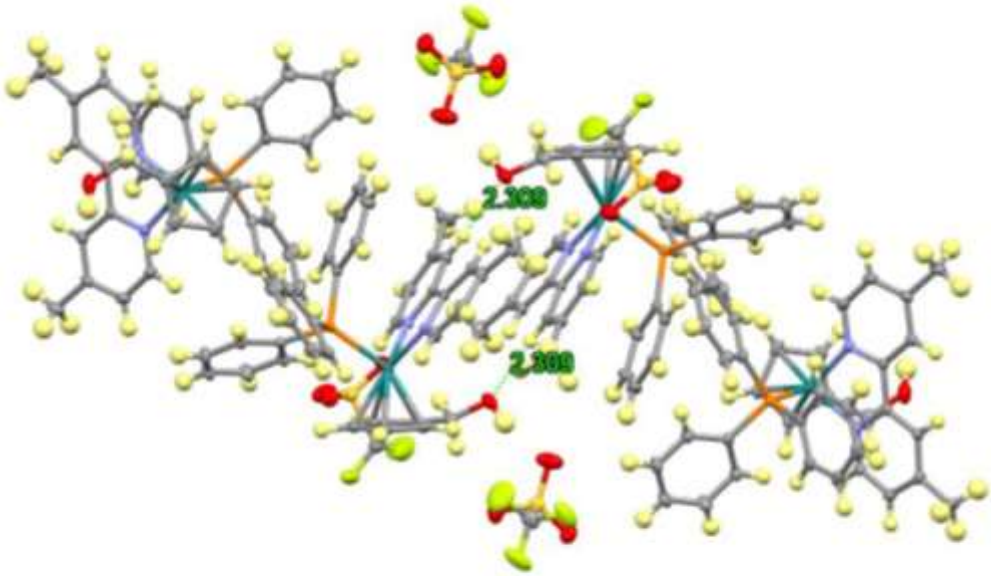

F)

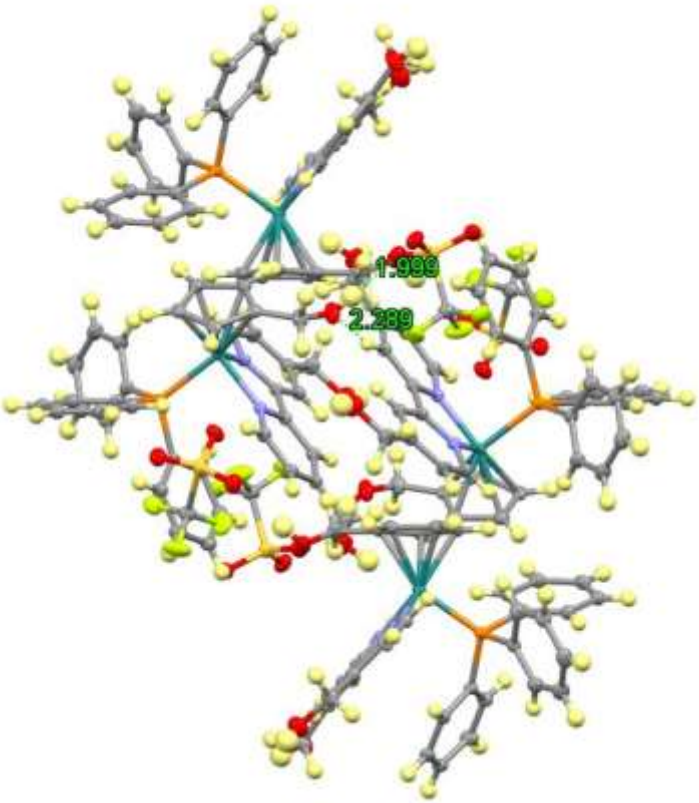

Figure S30. Packing diagram for complexes **1** (A), **2** (B), **3** (C), **5** (D), **6** (E) and **7** (F).

S5. Stability studies in aqueous solution

A) Compound 1

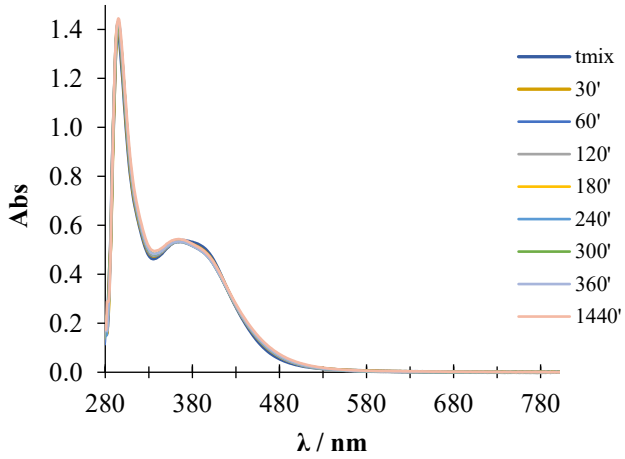

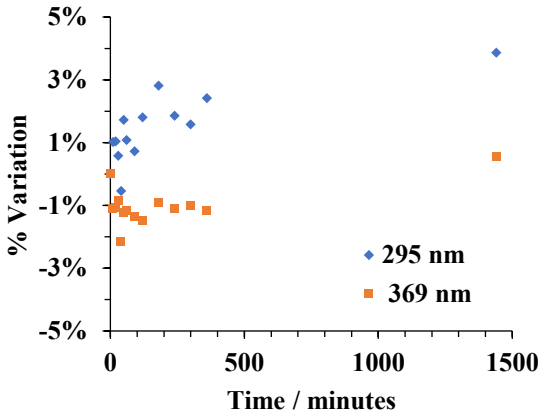

B) Compound 2

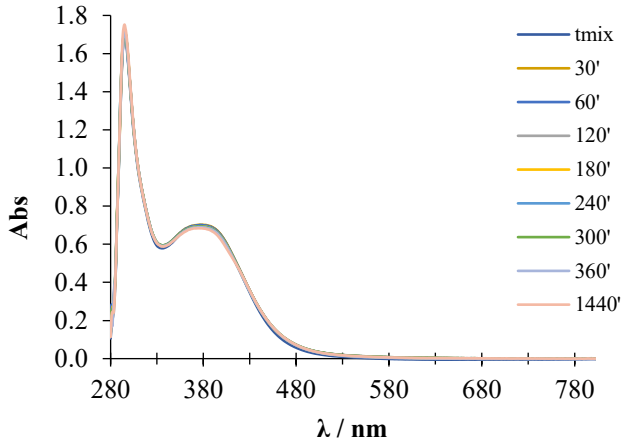

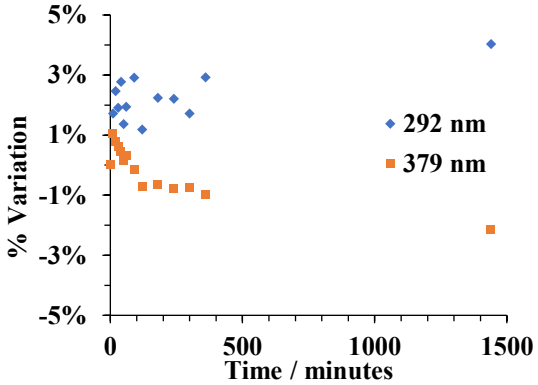

C) Compound 3

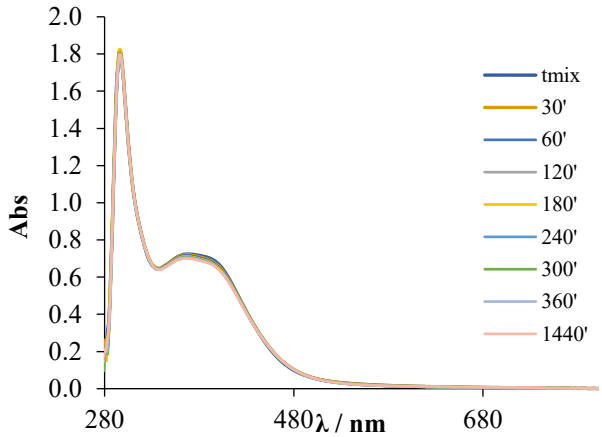

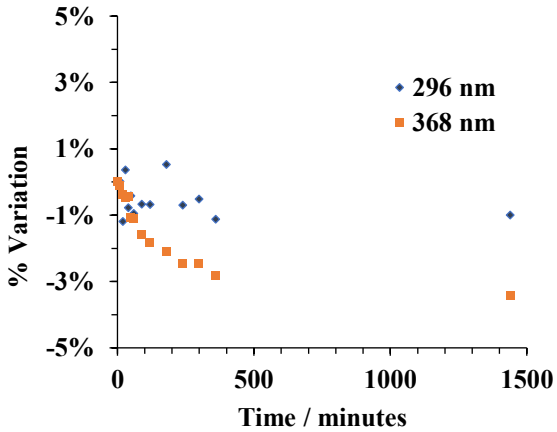

D) Compound 4

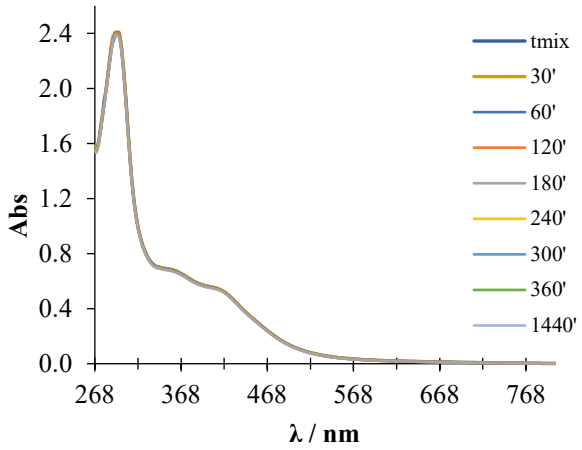

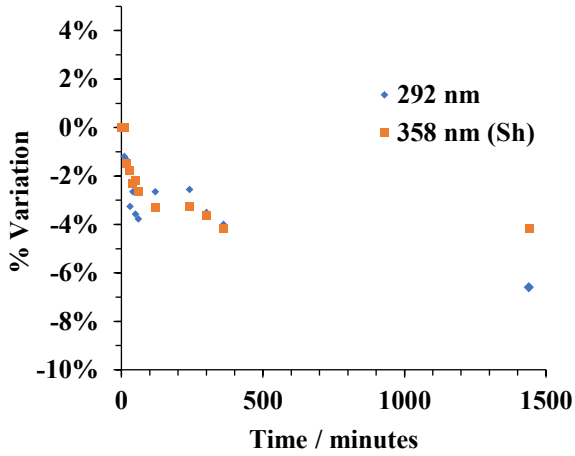

E) Compound 5

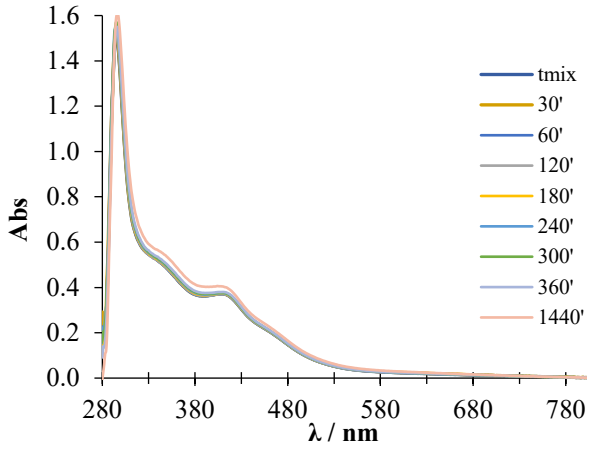

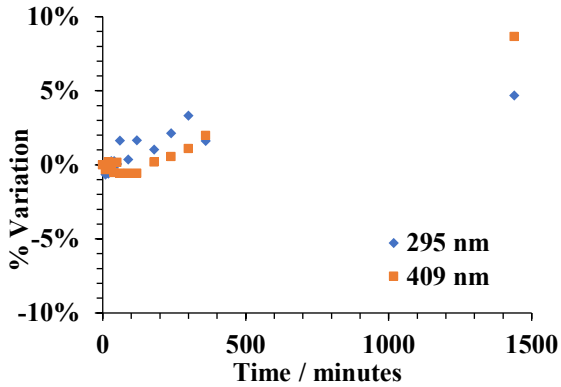

F) Compound 6

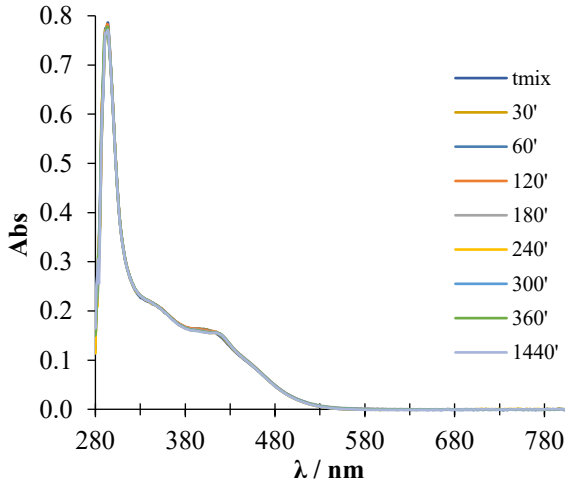

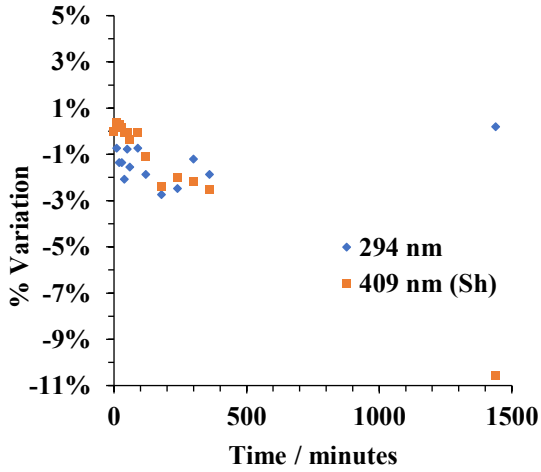

G) Compound 7

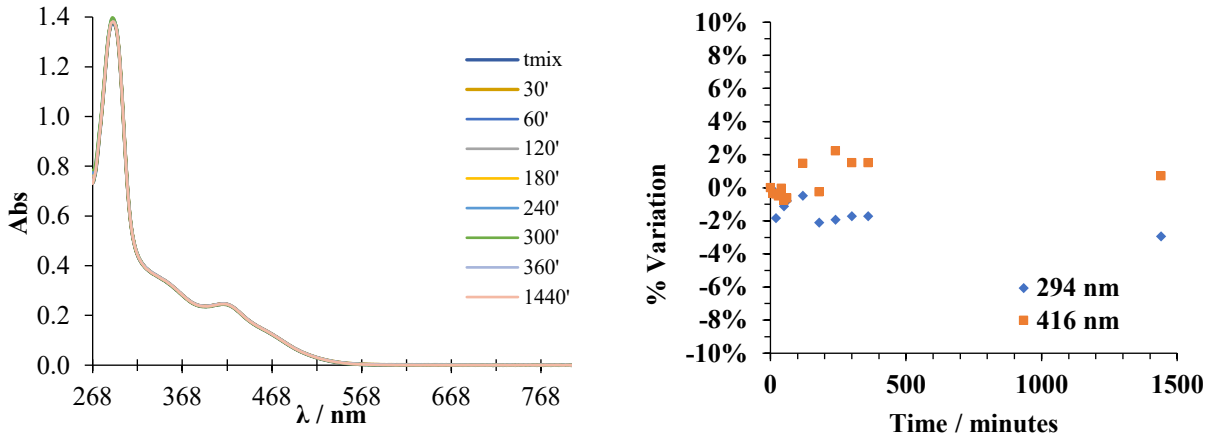

Figure S31. Stability studies in cellular media, 2% DMSO / 98 % DMEM for compounds **1** (A), **2** (B), **3** (C), **4** (D), **5** (E), **6** (F) and **7** (G). On the right are represented the UV-Vis spectra during the 24 h of the study and on the left the percentage of variation for fixed wavelengths along time (1 cm optical path; see experimental section for details).

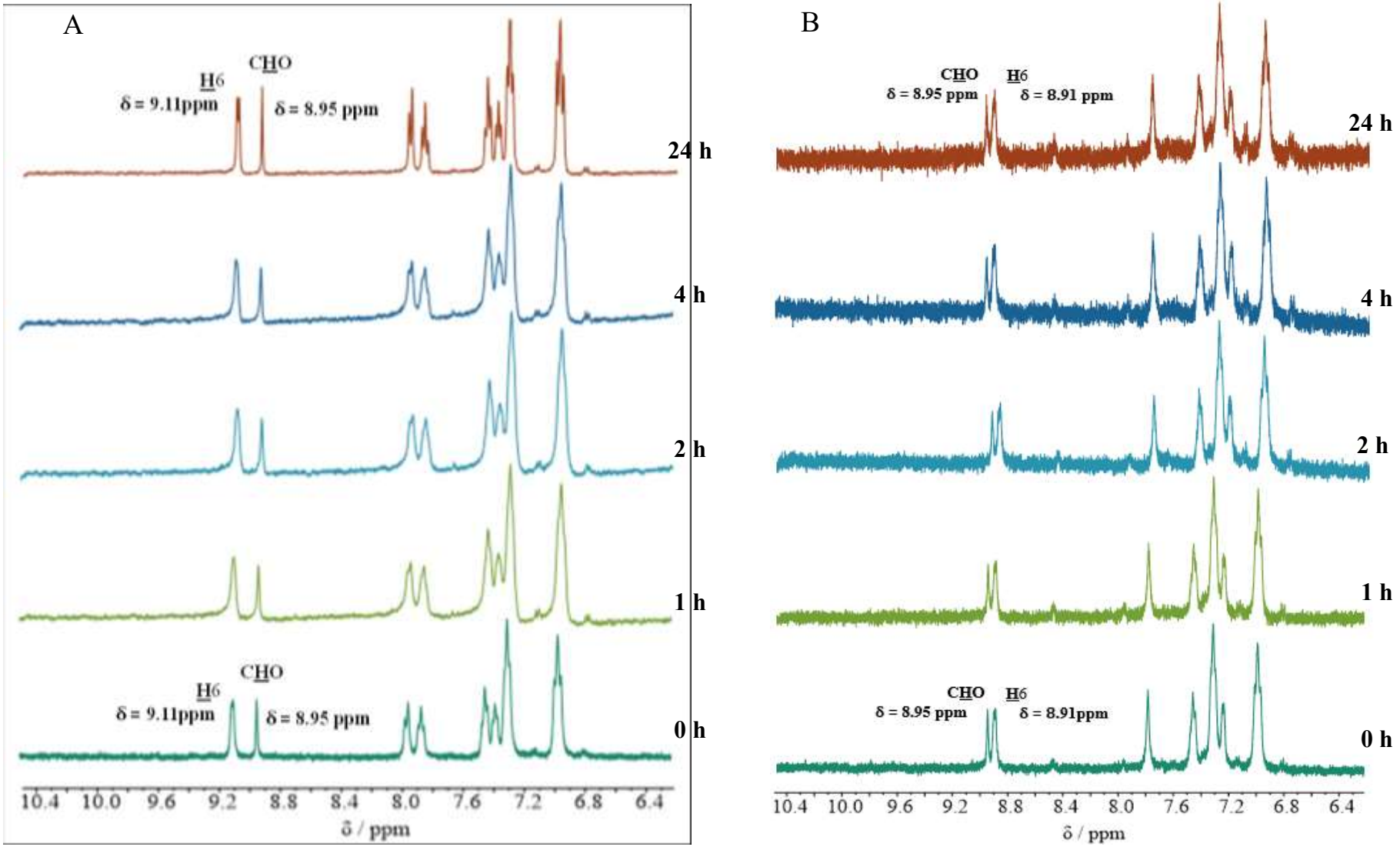
A
H6
δ = 9.11ppm
CHO
δ = 8.95 ppm
24 h
4 h
2 h
1 h
0 h
10.4 10.0 9.6 9.2 8.8 8.4 8.0 7.6 7.2 6.8 6.4
δ / ppm
B
CHO
δ = 8.95 ppm
H6
δ = 8.91 ppm
24 h
4 h
2 h
1 h
0 h
10.4 10.0 9.6 9.2 8.8 8.4 8.0 7.6 7.2 6.8 6.4
δ / ppm

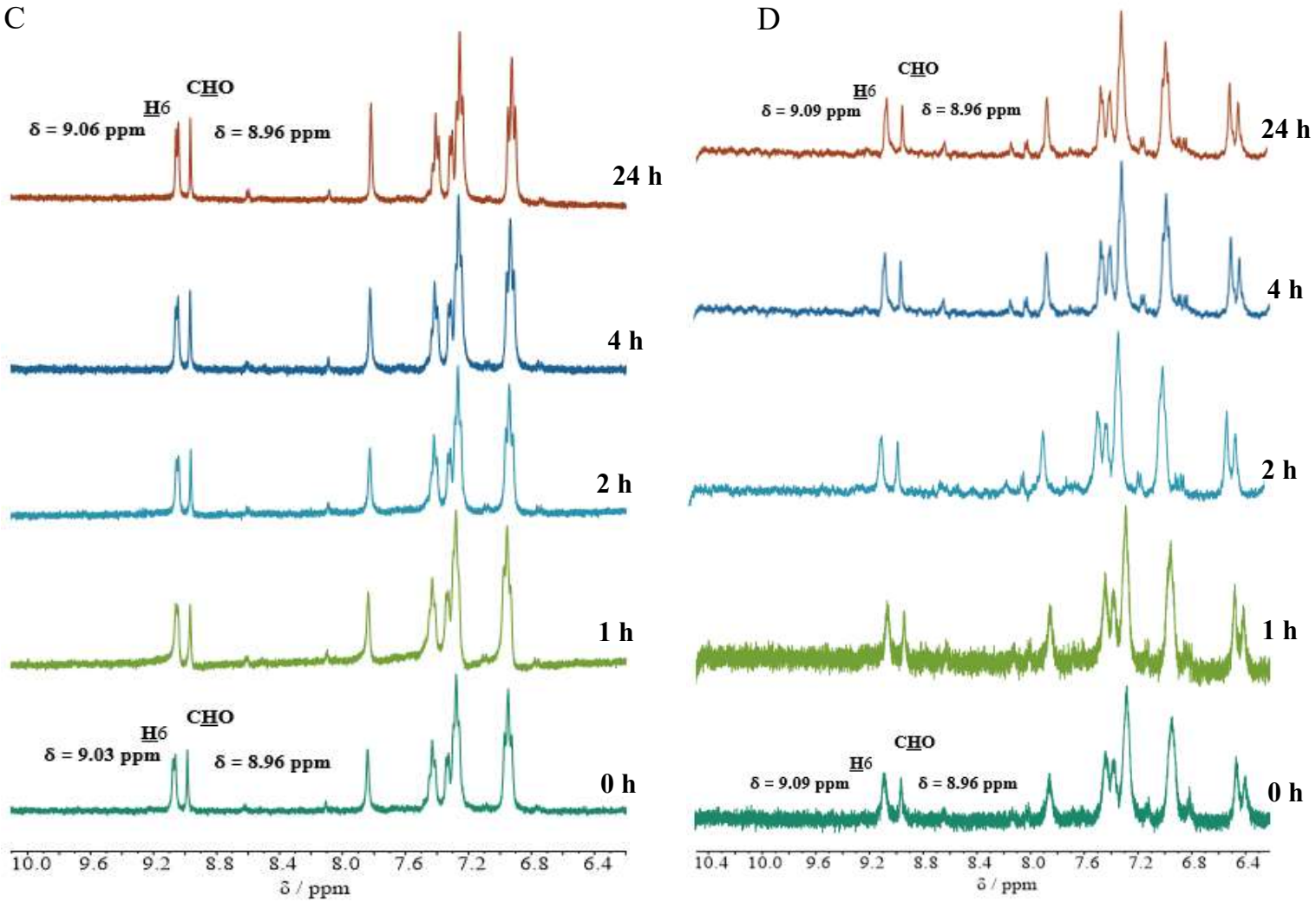

Figure S32. Stability studies monitored by ^{1}H-NMR in cellular media (35 % DMSO / 65 % DMEM) for compounds **1**(A), **2**(B), **3**(C) and **4**(D).

S6. P-gp and MRP1 expression in non-small cell lung cancer cell lines

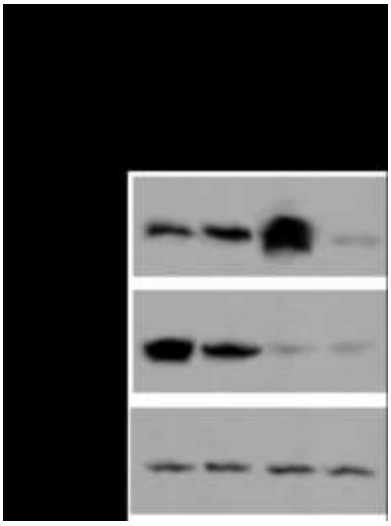

Figure S33. P-gp and MRP1 expression in non-small cell lung cancer cell lines, measured by immunoblotting. The figure is representative of 1 out of 3 experiments. Tubulin has been used to check the equal control of proteins.